The Determination of Wave Group Parameters from the Resolution of Incident and Reflected Waves

by
Gregory E. Selfridge

A project
submitted to the
Department of Civil Engineering
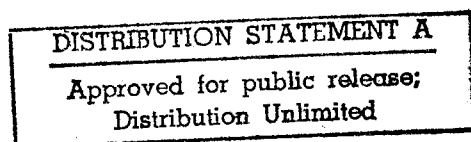Oregon State University
Corvallis, OR

N00123-89-G-0508

in partial fulfillment of
the requirements for
the degree of
Master of Science

19950428 031

March 9, 1995

ABSTRACT

Laboratory tests conducted to determine the effects of wave groups on rubble mound breakwater stability are analyzed. A literature review outlining the controversy regarding whether or not wave groups effect breakwater stability is given. Resolution of this controversy is proposed using two independent parameters that characterize wave groups. The two parameters are an envelope exceedance coefficient α and spectral shape γ. The incident time series must be known to compute α, and an algorithm is given that will resolve incident and reflected wave time series from closely spaced wave gauges. The digital to analog simulation of laboratory waves with specified wave group characteristics is reviewed. It is recommended that further studies be conducted to parameterize the envelope exceedance coefficient α with a non-biased groupiness factor.

Accesion For		
NTIS CRA&I	☒	
DTIC TAB	☐	
Unannounced	☐	
Justification *per form 50*		
By		
Distribution /		
Availability Codes		
Dist	Avail and / or Special	
A-1		

TABLE OF CONTENTS

INTRODUCTION

The design of rubble mound breakwaters is one of the oldest and most common applications of coastal engineering methodologies. Design of rubble mound structures is most commonly based on the empirical methods presented in the Shore Protection Manual (SPM 1984). Due to some failures of structures designed with the SPM methodology, an effort to improve the SPM design methodology is undertaken. The design methodology presented in the SPM is based on empirical formulas developed from experiments with monochromatic waves. Most of the more recently proposed design criteria are based on laboratory experiments using irregular waves. The effects of spectral shape and wave grouping will be targeted. As a proposed improvement, factors such as permeability, wave period, and storm duration may have secondary effects on rubble mound breakwater stability.

It has been well-documented that waves in random seas tend to form groups not accounted for by the purely Gaussian random wave model. Many of the coastal engineering problems associated with wave groups have been documented by Medina and Hudspeth (1990). In the last two decades, controversy has arisen as to whether spectra composed of grouped waves cause different levels of damage to rubble mound structures than spectra of ungrouped waves. Medina et al. (1990) have found that most of the controversy may be resolved if two independent spectral related parameters are chosen to characterize the wave groups (Mase and Iwagaki 1986). One parameter characterizes the length of wave groups and the other characterizes the magnitude of the

energy flux in a group of waves.

Intermediate scale laboratory studies to determine if wave groups affect rubble mound breakwater stability were performed in the 2-dimensional wave channel at the O. H. Hindsdale Wave Research Facility (OHH-WRF) at Oregon State University. In order to determine the effects of wave groups on rubble mound structures, sea states with identical amplitude spectra but different wave group characteristics were simulated. The resolution of incident and reflected wave time series from the random wave simulation is required in order to evaluate the effects of wave groups. In order to quantify the two wave group characteristics proposed by Mase and Iwagaki (1986), the incident time series must be known. Medina et al. (1994) used a method developed by Kimura (1985) and Fassardi (1993) that extends an algorithm proposed by Goda and Suzuki (1976) to resolve the incident and reflected wave time series from closely spaced wave gauges.

CHAPTER I: Correlation of Wave Groups with Armor Damage

Carstens, et al. (1967), first observed the effect of wave groups on breakwater damage when he analyzed two time series with significantly different groupiness, but similar spectra and wave statistics. The time series with the more grouped waves, taken from a field site in the Barents Sea, created more damage than the time series generated from the theoretical Neumann-spectrum. Johnson, et al. (1978), as a result of their laboratory studies on the effects of wave grouping on breakwater stability, concluded that wave grouping was an essential parameter in the model testing of rubble mound breakwater stability. Wave trains with similar spectra and wave statistics, but different groupiness, caused significantly different levels of damage, the greater damage being caused by the grouped wave trains. Burcharth (1979) also concluded that wave grouping, or the succession of the waves, is important in model design.

Since the energy spectrum does not contain the phases of the individual wave components in the sea surface it is necessary to also resolve the phases of the individual wave components to reproduce an accurate succession of wave heights (Rye 1982). In his summary of breakwater design, Bruun (1989) recorded that the resolution of the phase spectrum identified apparent order where none is assumed in the Gaussian random wave model. He concluded that these ordered wave groups are more damaging than other waves.

In contrast, van der Meer (1988) found that the spectral shape and grouping of waves had little or no influence on the stability of breakwater armor layers provided that

the average spectral period was used to simulate the sea state rather than the peak period. Hall (1994), in a study on bermed breakwaters, concluded that wave groups are only important during the stage of incipient motion, and that once motion is initiated wave groupiness is no longer important.

Medina et al. (1990) found that much of the controversy could be resolved if the two independent parameters of wave groups proposed by Mase and Iwagaki (1986) were considered. One parameter measures the run length or the number of high waves in a time series, and a second parameter quantifies the magnitude of the variation of wave energy. In their laboratory tests, Medina et al. (1990) tested four different wave height time series proposed by Mase and Iwagaki (1986) shown in Figure 1.1, while keeping other secondary factors that affect breakwater stability constant.
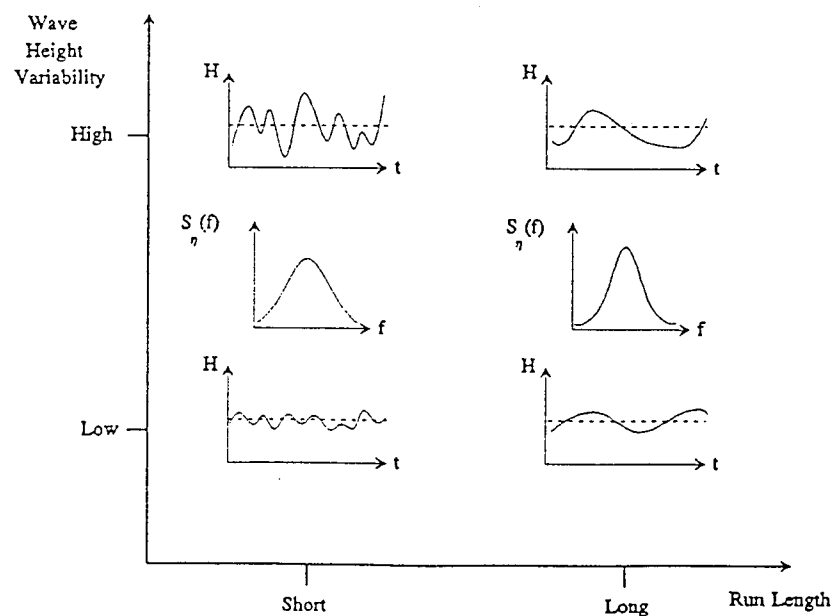

Figure 1.1 - Classification of wave height time series (Fassardi 1993)

4

Figure 1.1 shows that identical spectra may have different magnitudes of wave height variability, which may cause different levels of damage. Likewise, different spectra may have the same magnitude of wave height variability, and thus cause the same level of damage. Medina et al. (1990) simulated truncated Goda-JONSWAP spectra with different run lengths and different magnitudes of variation of wave energy according to Appendix B.

Medina et al. (1990) concluded that the spectral shape and run length alone were not sufficient parameters to accurately describe wave groupiness, but that another parameter that measured the variation of wave energy more completely described the wave group. Medina et al. (1990) correlated an envelope exceedance coefficient α that measures the variation of wave energy with stability, and demonstrated that random wave trains with the same spectral shape may produce different levels of damage. Medina et al. (1994) found no significant correlation between the spectral peakedness γ and armor damage, but concluded that the envelope exceedance coefficient α was necessary to evaluate the effects of random waves on structures in both physical and prototypical models.

CHAPTER II: Derivation of Envelope Exceedance Coefficient α

From their analysis of storm waves, Mase and Iwagaki (1986) recommended using at least two parameters to quantify wave groups, one parameter that measures the magnitude of a sequence of high waves in a time series, and a second parameter that measures the magnitude of the variation of wave energy. Both parameters are shown schematically in Figure 2.1, where A(x,t) is the wave envelope function from the Hilbert transform defined by Medina and Hudspeth (1990).
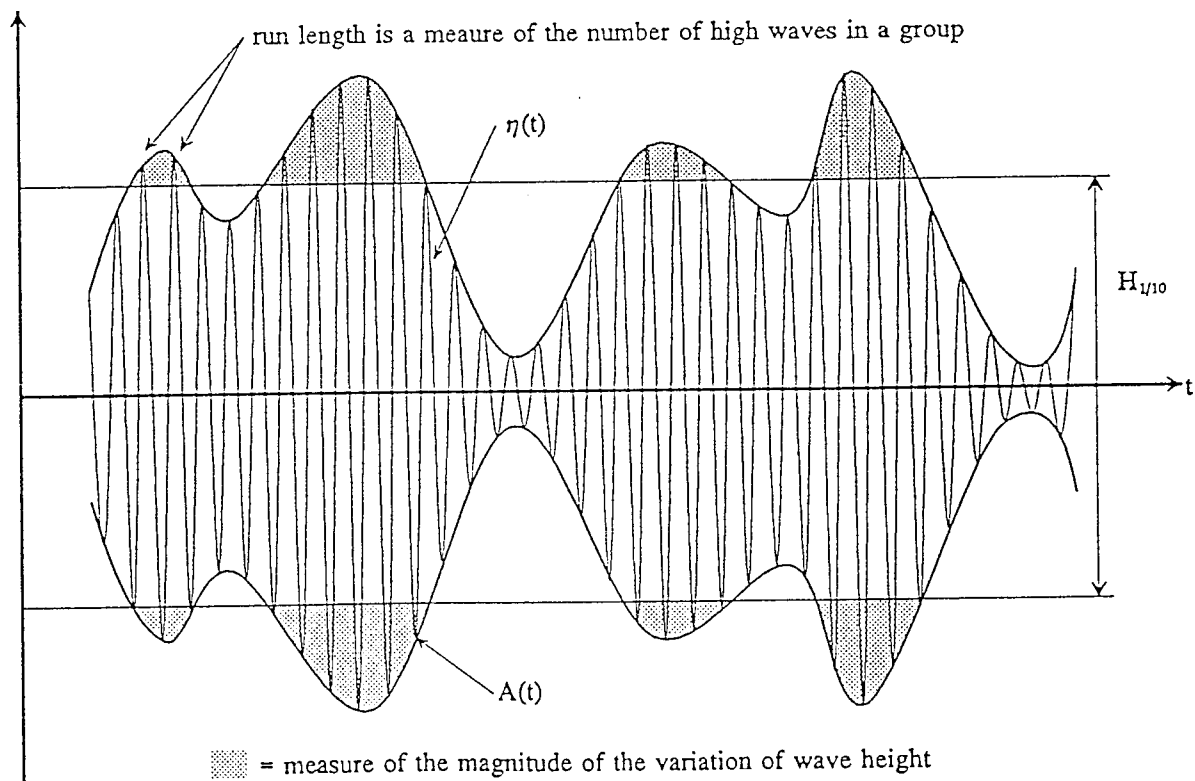

Figure 2.1 - Wave group parameters

The peak enhancement factor γ of the Goda-JONSWAP spectrum (Goda 1985) controls the sharpness of the spectral peak and was selected to characterize the magnitude of the sequence of high waves in the time series. Rye (1980) related the magnitude of the sequence of high waves, run length, to the peak enhancement factor γ of the JONSWAP spectrum. The coefficient α was selected to characterize the magnitude of variation of wave energy. The envelope exceedance coefficient α is a dimensionless measure of the wave energy exceeding that associated with a prescribed wave height; e. g., $H_{1/10}$.

In a two dimensional wave channel, the wave height function $H(x,t)$ is defined by

$$H(x,t) = 2A(x,t) \qquad (2.1)$$

If Δt = a constant sampling time interval, the discrete wave height function at a fixed location may be expressed as $H(n\Delta t)$. Defining a normalized measure of the variation of wave height as

$$\Delta H_n = \frac{H(n\Delta t)}{H_{1/10}} - 1 \qquad (2.2)$$

and the Heaviside step function (Farlow 1982) of ΔH_n as

$$U(\Delta H_n) = \left\{ \begin{array}{ll} 0 & \Delta H_n < 0 \\ 1 & \Delta H_n \geq 0 \end{array} \right. ; \qquad (2.3)$$

then the magnitude of the variation of wave energy above $H_{1/10}$ of the time series is given as

7

$$\alpha' = \frac{1}{N} \sum_{n=1}^{N} (\Delta H_n)^2 U(\Delta H_n) \tag{2.4}$$

where N is the number of discrete data points in the time series. Normalizing Eq. (2.4) by the expected value of α' yields the envelope exceedance coefficient α defined as

$$\alpha = \frac{\alpha'}{E[\alpha']} \tag{2.5}$$

where $E[\alpha']$ is defined as

$$E[\alpha'] = \int_{H_{1/10}}^{\infty} \left[\frac{H}{H_{1/10}} - 1 \right]^2 p(H) \; dH \tag{2.6}$$

where H is the wave height function at a fixed location H(t), and p(H) is the Rayleigh probability density function of H(t) (Appendix A) defined by Chakrabarti (1987) as

$$p(H) = \frac{H}{4m_0} \exp \left[\frac{-H^2}{8m_0} \right] \tag{2.7}$$

and m_0 is the variance of the time series. If the following substitution is made (Sarpkaya and Isaacson 1981),

$$H_{1/10} = 5.091 \sqrt{m_0} \tag{2.8}$$

Eq. (2.6) may be solved numerically to obtain $E[\alpha'] = 0.001346$.

8

CHAPTER III: Resolution of Incident and Reflected Wave Time Series

In order to determine experimental wave heights and to calculate envelope exceedance coefficients, the incident time series must be known. Because of reflection from models in a 2-dimensional wave channel, a method to resolve the incident and reflected random wave time series from wave gauges must be used. Bad data points in wave records caused by wave gauge malfunction are smoothed using the FORTRAN program CLEANREC that employs a smoothing spline package developed by H. J. Woltring (1986). A Fast Fourier Transform (FFT) analysis is used to compute the raw wave spectrum from which the incident and reflected random wave time series may be determined. Goda and Suzuki (1976) modified a method developed by Thornton and Calhoun (1972) to resolve the incident and reflected wave spectra from wave gauges spatially separated by a distance $\Delta\ell$ (see Fig. 3.1).
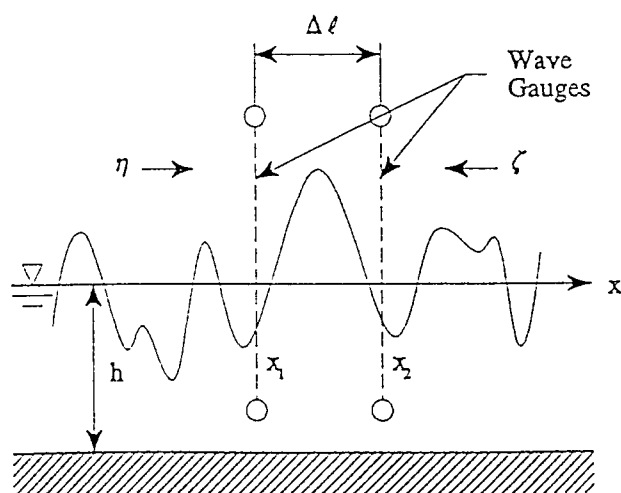

Figure 3.1 - Definition Sketch for two wave gauges

Kimura (1985) and Fassardi (1993) extended the Goda and Suzuki algorithm to include wave phases so that incident and reflected time series could be resolved.

Goda and Suzuki (1976) analyzed two simultaneous wave records recorded by closely spaced wave gauges aligned in the direction of wave propagation by an FFT. If the incident η and reflected ζ random wave time series at the ith wave gauge at frequency ω are given by

$$\eta_i = a \, \cos(kx_i - \omega t + \varepsilon) \tag{3.1a}$$

$$\zeta_i = b \, \cos(kx_i + \omega t + \beta) \tag{3.1b}$$

then the wave profile at the ith wave gauge may be expressed as

$$(\eta_i + \zeta_i)_{(x = x_i)} = A_i \cos\omega t + B_i \sin\omega t \tag{3.2}$$

where

$$A_1 = a \, \cos\psi_I + b \, \cos\psi_R \tag{3.3a}$$

$$B_1 = a \, \sin\psi_I - b \, \sin\psi_R \tag{3.3b}$$

$$A_2 = a \, \cos(k\Delta\ell + \psi_I) + b \, \cos(k\Delta\ell + \psi_R) \tag{3.3c}$$

$$B_2 = a \, \sin(k\Delta\ell + \psi_I) - b \, \sin(k\Delta\ell + \psi_R) \tag{3.3d}$$

where the spatial phases of the incident and reflected waves, respectively, are defined as

$$\psi_I = kx_1 + \varepsilon \tag{3.4a}$$

$$\psi_R = kx_1 + \beta \tag{3.4b}$$

$$x_2 = x_1 + \Delta\ell \tag{3.4c}$$

and x_1 and x_2 are the wave gauge positions as shown in Figure 3.1. The coefficients A_i

and B_i may be related to the complex-valued FFT coefficient X by (Dean and Dalrymple 1984)

$$X = \frac{A_i - jB_i}{2} \tag{3.5}$$

where $j = \sqrt{-1}$. Goda and Suzuki (1976) solve Eqs. (3.3) simultaneously for estimates of the amplitudes a and b listed in Table 3.1.

For irregular waves, the time series are the superposition of many wave components given by Eqs. (3.1). Because Eqs. (3.3) apply to each Fourier component in an irregular wave record, linear superposition may be used to resolve time series from a spectrum of Fourier components (Goda 1985). Goda and Suzuki (1976) observed that spectral estimates diverged (toward infinity) near frequencies satisfying the condition $k\Delta\ell = n\pi$ for $n = 0, 1, 2, \ldots$, because the term $|\sin k\Delta\ell|$ in the denominator of the equations for the amplitudes a and b in Table 3.1 becomes small and errors from noise are amplified. Therefore, the wave gauge spacing $\Delta\ell$ determined the frequency limits of a band pass filter from which the waves could be separated into incident and reflected time series. The wave amplitudes a and b could be resolved effectively for the interval $0.1\pi \leq k\Delta\ell \leq 0.9\pi$. Goda and Suzuki (1976) recommended the following effective band pass limits for experimental conditions:

$$0.05L_{max} \leq \Delta\ell \leq 0.45L_{min} \tag{3.6a}$$

where L_{max} and L_{min} denote the wavelengths corresponding to the lower (f_{min}) and upper (f_{max}) frequency limits, respectively, of the band pass filter. Goda and Suzuki (1976) note

that the effective range may be taken slightly wider than given in Eq. (3.6a) such that

$$0.03L_{max} \leq \Delta\ell \leq 0.45L_{min}$$ (3.6b)

Goda and Suzuki (1976) also recommended that the wave gauges be located at least one wavelength away from both the breakwater toe and the wave generator.

Kimura (1985) extended the Goda and Suzuki algorithm to include situations where each incident wave component in the Fourier spectrum results in a different reflection coefficient from the structure. Kimura (1985) defined incident and reflected wave profiles by Eqs. (3.1), and the spatial phases by Eqs. (3.4a,b). Eqs. (3.1) are similar to Kimura's Eqs. (9 & 12) on pages 62-63 (1985) if the sign of the temporal term is changed from minus to plus in his Eq. (12). Kimura (1985) also solved for the spatial wave phases defined in Eqs. (3.4a,b). Values for a, b, ψ_I, and ψ_R may be calculated using the equations listed in Table 3.1 for Kimura. To improve the resolution of incident and reflected waves, Kimura recommended a slightly more conservative data window of

$$0.15L_{max} \leq \Delta\ell \leq 0.35L_{min}$$ (3.7)

Fassardi (1993) followed the approach of Kimura (1985) to extend the Goda and Suzuki algorithm (1976). However, he defined the incident η and reflected ζ time series at the ith wave gauge as

$$\eta_i = a \, \cos(kx_i - \omega t - \varepsilon)$$ (3.8a)

$$\zeta_i = b \, \cos(kx_i + \omega t + \beta)$$ (3.8b)

If the spatial phase of the incident and reflected waves, respectively, are defined as

$$\psi_I = kx_1 - \varepsilon$$ (3.9a)

12

$$\psi_R = kx_1 + \beta \tag{3.9b}$$

rather than by Eqs. (3.4a,b), then the amplitudes and spatial phases are given by the equations listed in Table 3.1 for Fassardi (1993). The only difference between the Fassardi and Kimura algorithm is the sign of ε in the definition of the incident time series phase. This sign change results in corresponding sign changes in the Fourier coefficients that are now given by

$$A_1 = a \cos\psi_I + b \cos\psi_R \tag{3.10a}$$

$$B_1 = a \sin\psi_I + b \sin\psi_R \tag{3.10b}$$

$$A_2 = a \cos(-k\Delta\ell + \psi_I) + b \cos(k\Delta\ell + \psi_R) \tag{3.10c}$$

$$B_2 = a \sin(-k\Delta\ell + \psi_I) + b \sin(k\Delta\ell + \psi_R) \tag{3.10d}$$

These four equations are then solved simultaneously to obtain the equations for a, b, ψ_I, and ψ_R listed in Table 3.1 for Fassardi (1993).

In the experiments documented by Medina et al. (1994), the Fassardi algorithm was used to resolve the incident and reflected time series. Three sonic wave gauges aligned in the direction of wave propagation were centered 10m from the toe of the breakwater and spatially separated by $\Delta\ell = 1.22$m according to Figure 3.2.

Clean time series from each gauge were used in the FORTRAN program RECANSYG to resolve the incident and reflected time series. RECANSYG outputs the raw time series and spectra resolved from the wave gauge system in Figure 3.2. The program computes the time series mean and variance. As well, it computes the reflection coefficient, significant wave height, and mean period from the moments. The

13

Goda and Suzuki (1976)	$a = \dfrac{1}{2\,\lvert \sin k\Delta\ell \rvert}\sqrt{(A_2 - A_1\cos k\Delta\ell - B_1\sin k\Delta\ell)^2 + (B_2 + A_1\sin k\Delta\ell - B_1\cos k\Delta\ell)^2}$ $b = \dfrac{1}{2\,\lvert \sin k\Delta\ell \rvert}\sqrt{(A_2 - A_1\cos k\Delta\ell + B_1\sin k\Delta\ell)^2 + (B_2 - A_1\sin k\Delta\ell - B_1\cos k\Delta\ell)^2}$
Kimura (1985)	$a = \dfrac{1}{2\,\lvert \sin k\Delta\ell \rvert}\sqrt{(A_2 - A_1\cos k\Delta\ell - B_1\sin k\Delta\ell)^2 + (B_2 + A_1\sin k\Delta\ell - B_1\cos k\Delta\ell)^2}$ $b = \dfrac{1}{2\,\lvert \sin k\Delta\ell \rvert}\sqrt{(A_2 - A_1\cos k\Delta\ell + B_1\sin k\Delta\ell)^2 + (B_2 - A_1\sin k\Delta\ell - B_1\cos k\Delta\ell)^2}$ $\psi_I = \tan^{-1}\left[\dfrac{-A_2 + A_1\cos k\Delta\ell + B_1\sin k\Delta\ell}{B_2 + A_1\sin k\Delta\ell - B_1\cos k\Delta\ell}\right]$ $\psi_R = \tan^{-1}\left[\dfrac{-A_2 + A_1\cos k\Delta\ell - B_1\sin k\Delta\ell}{-B_2 + A_1\sin k\Delta\ell + B_1\cos k\Delta\ell}\right]$
Fassardi (1993)	$a = \dfrac{1}{2\,\lvert \sin k\Delta\ell \rvert}\sqrt{(A_2 - A_1\cos k\Delta\ell + B_1\sin k\Delta\ell)^2 + (B_2 - A_1\sin k\Delta\ell - B_1\cos k\Delta\ell)^2}$ $b = \dfrac{1}{2\,\lvert \sin k\Delta\ell \rvert}\sqrt{(A_2 - A_1\cos k\Delta\ell - B_1\sin k\Delta\ell)^2 + (B_2 + A_1\sin k\Delta\ell - B_1\cos k\Delta\ell)^2}$ $\psi_I = \tan^{-1}\left[\dfrac{-A_2 + A_1\cos k\Delta\ell - B_1\sin k\Delta\ell}{B_2 - A_1\sin k\Delta\ell - B_1\cos k\Delta\ell}\right]$ $\psi_R = \tan^{-1}\left[\dfrac{-A_2 + A_1\cos k\Delta\ell + B_1\sin k\Delta\ell}{B_2 + A_1\sin k\Delta\ell - B_1\cos k\Delta\ell}\right]$

Table 3.1 - Summary of incident and reflected wave amplitudes and phases

incident and reflected time series were resolved using Gauges 1 and 2 *and* Gauges 2 and 3 so that the algorithm could be verified by duplication. A sample run is analyzed. As explained in APPENDIX B - Simulation of Sea States, Run E1P1L7 represents a sea state simulated with the following parameters:

E1 = Envelope 1 ; $\gamma=10, \alpha=2.52$

P1 = Phase 1 ; $\phi=2\pi/3$
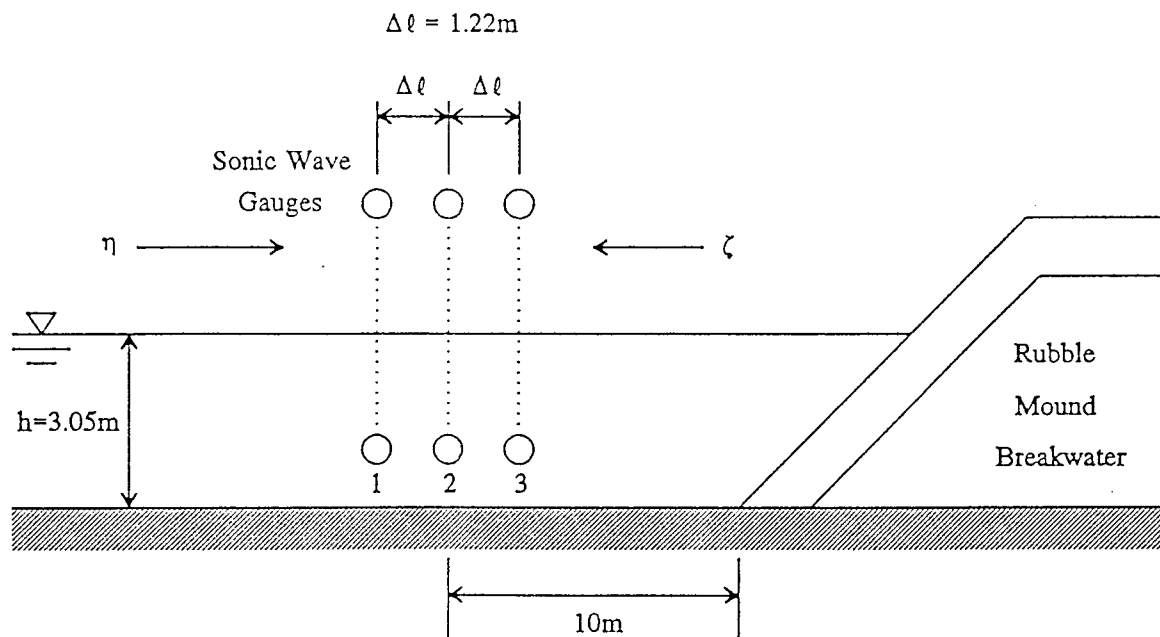
L7 = Height 7 ; $H_{s(7)}=0.723$

$\Delta\ell = 1.22m$

Figure 3.2 - Sonic Wave Gauge Locations (Fassardi 1993)

For a small data sample of ten seconds, Figure 3.3 shows how the clean time series are phase shifted at each wave gauge station. Figure 3.4 shows two minutes of the

clean time series at Gauges 1 and 2 and the resulting incident and reflected time series resolved by the Fassardi (1993) algorithm. The time series at Gauge 1 is identical to that at Gauge 2, except for the phase shift. The incident and reflected time series resolved from Gauges 1 and 2 are plotted on the same scale to show the relative magnitude of the incident and reflected wave amplitudes. The magnitude of the wave amplitudes of the reflected time series are about 25% of the incident amplitudes. Figure 3.5 shows the composite spectrum at Gauge 2 and the incident and reflected spectra resolved from Gauges 1 and 2 *and* Gauges 2 and 3, respectively. The spectra in Figure 3.5 have been smoothed using the non-statistical technique Box Car Averaging. The resolved spectra show that the energy in the reflected spectrum is about 5-10% of that in the incident spectrum. Breakwater reflection of about 25% observed in the time series results in the reflected spectral density being 5-10% of the incident spectral density, for each frequency component. The low frequency spike in the spectral density at approximately 0.04 Hz is attributed to a seiche in the wave channel caused by the start-up of the wave generator. The resolved spectra in Figure 3.5 are similar, indicating that the Fassardi (1993) algorithm produces the same spectra from different wave gauge pairs. At the truncation limits of 0.2140 Hz and 0.7644 Hz, the spectral density of the incident and reflected waves begins to diverge because the term $|\sin k\Delta\ell|$ in the denominator of the equation for the amplitudes a and b in the Fassardi algorithm becomes small. Further examples of the resolution of incident and reflected time series and spectra from the output of RECANSYG for the four envelopes discussed in APPENDIX B are included in APPENDIX C - Time Series and Spectra.
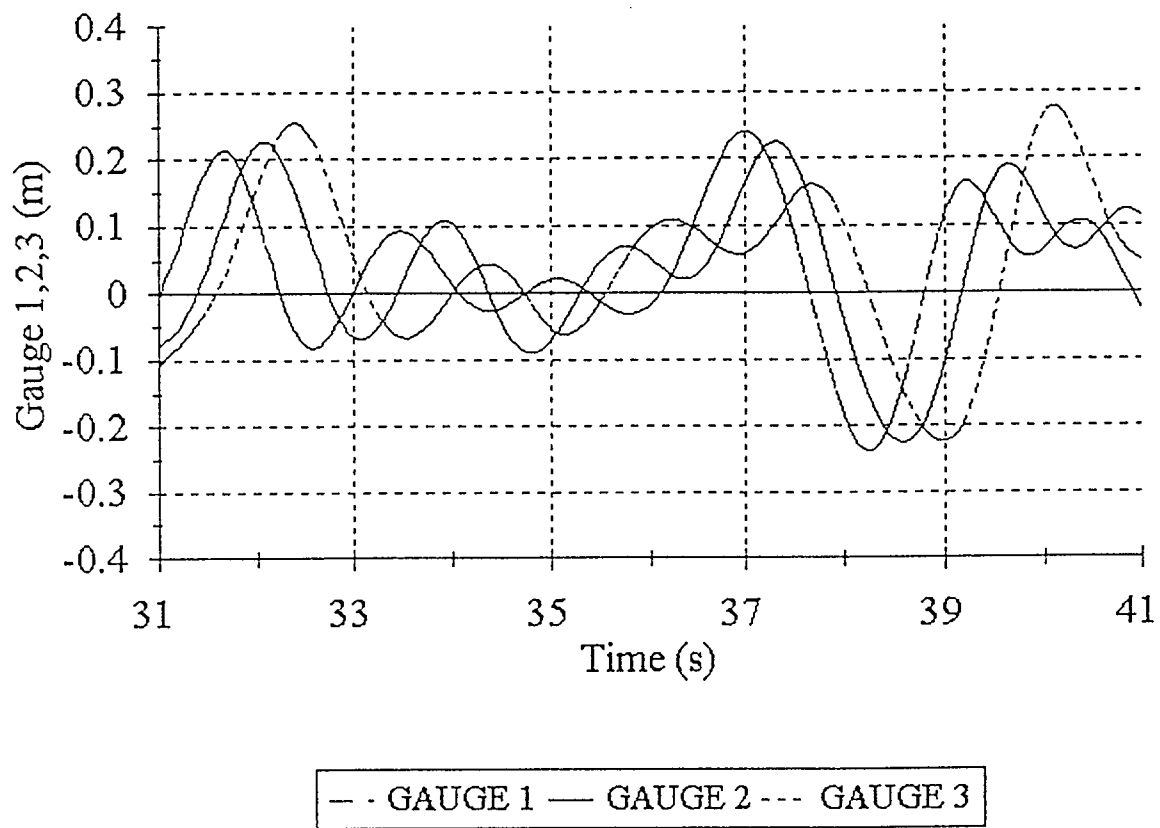
Time Series - Run E1P1L7

Figure 3.3 - Phase lag between time series at three wave gauges

Time Series – Run E1P1L7

Time Series – Run E1P1L7

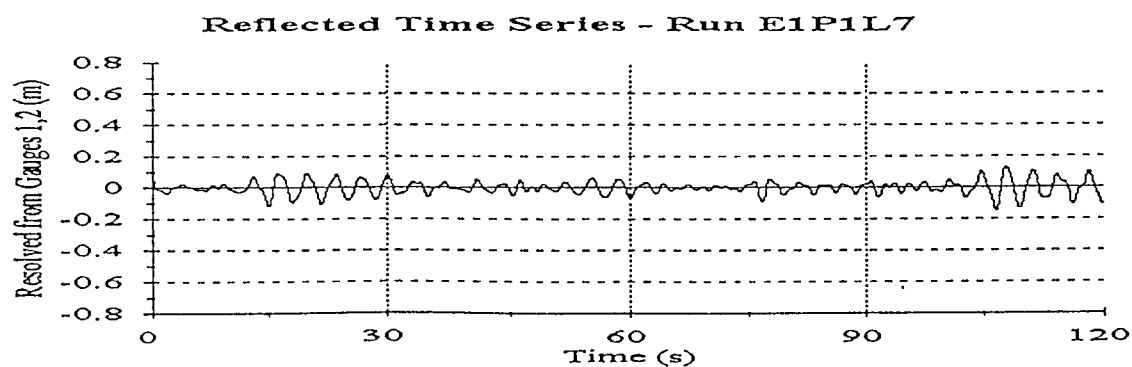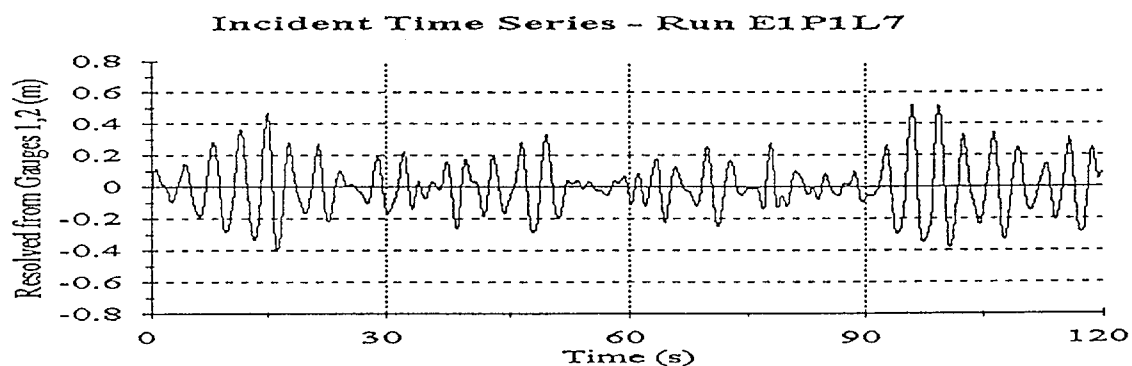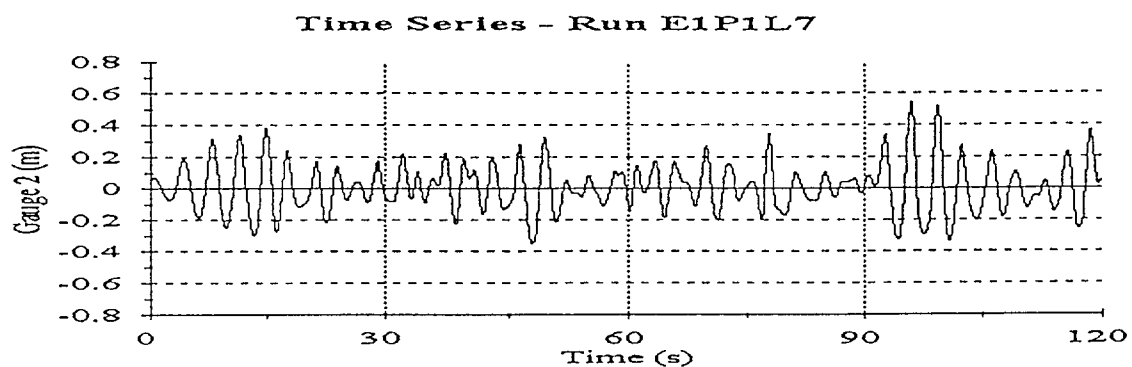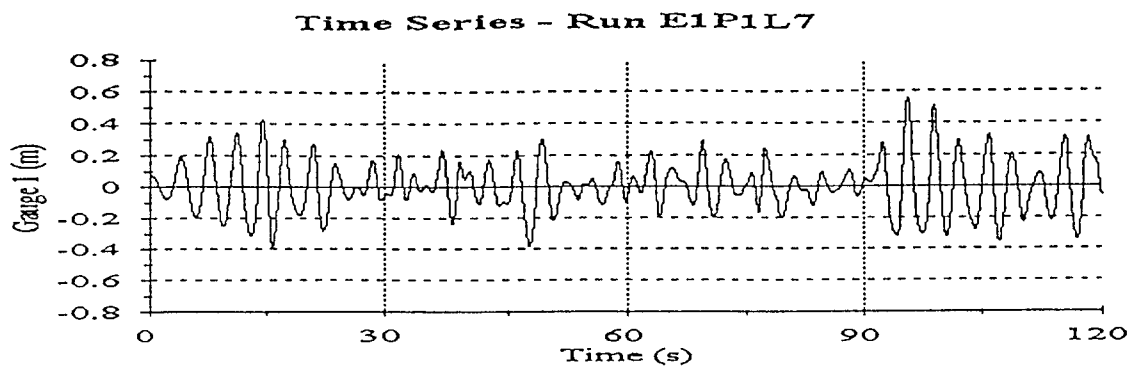**Incident Time Series – Run E1P1L7**

Reflected Time Series – Run E1P1L7

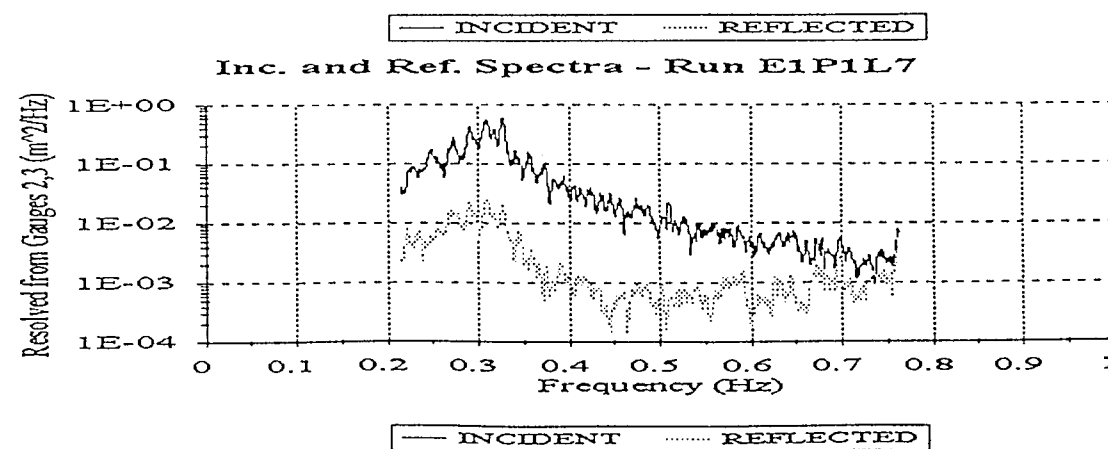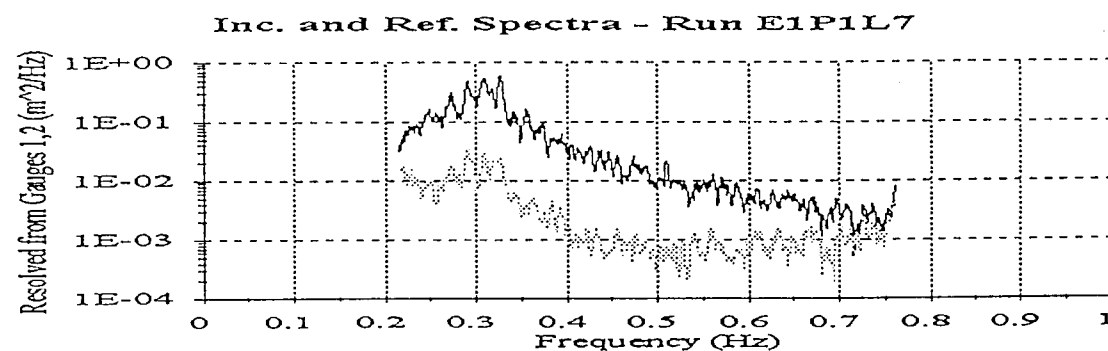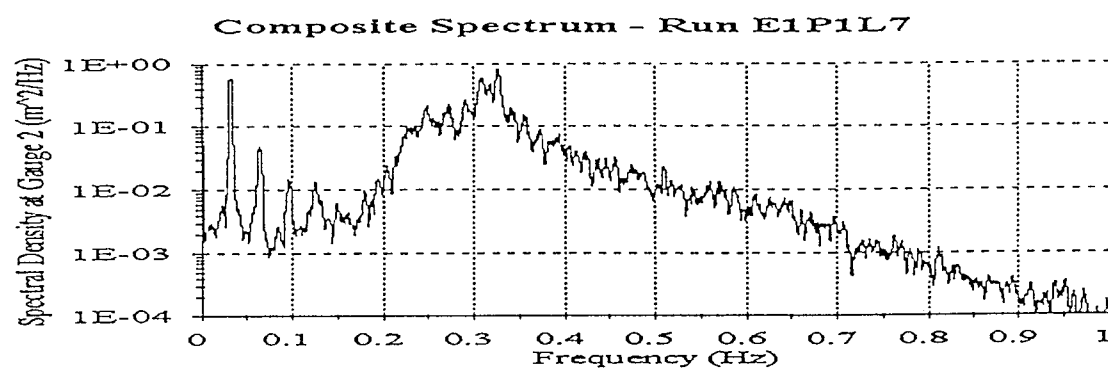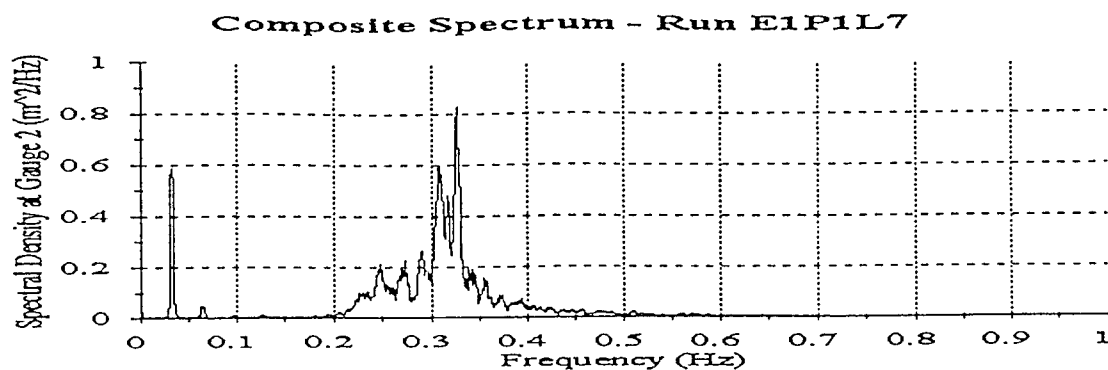Figure 3.4 – Time series resolved from Gauge 1 and 2

18

Figure 3.5 - Composite and Resolved Spectra

19

SUMMARY AND CONCLUSIONS

Multiple failures of existing rubble mound breakwaters designed with the Shore Protection Manual's (1984) methodology have indicated a need to improve the design procedures for rubble mound structures. Many structural and environmental characteristics such as armor grading, structure permeability, wave period, storm duration, spectral shape, and wave groupiness have secondary effects on breakwater stability. Irregular waves generated solely from an energy spectrum with random phases do not accurately model real wave trains, and the succession of wave heights or groupiness is an important factor in the design of rubble mound breakwaters. The magnitude of the energy flux given by the envelope exceedance coefficient α is one way of quantifying the groupiness of a wave time series. Intermediate scale wave channel studies at Oregon State University documented by Medina et al. (1990), Fassardi (1993), and Medina et al. (1994) have demonstrated that the envelope exceedance coefficient α may be used to correlate wave groupiness with breakwater damage. No significant correlation was found between the peak enhancement factor γ and rubble mound breakwater stability. Furthermore, the constant phase shift ϕ applied to the time series for each wave envelope $A(x,t)$ did not effect the armor damage.

To calculate the envelope exceedance coefficient α from the incident wave time series, either the Kimura (1985) or the Fassardi (1993) algorithm may be used to resolve the incident and reflected waves from closely spaced wave gauges. The Fassardi (1993) algorithm, used by Medina et al. (1990) in their experiments at Oregon State University

is different from the Kimura (1985) algorithm by the sign of the random phase angle of the incident time series (Eq. 3.1a & 3.8a). This sign change does not have any effect on the value of α or the interpretation of the results. For the frequency range given by Table B.1, the Fassardi (1993) algorithm effectively resolves incident and reflected wave time series from closely spaced wave gauges aligned in the direction of wave propagation. Some divergence of the incident and reflected wave spectra is observed near the cut off frequencies of the truncated spectra.

Since the wave resolution algorithms presented only resolve wave components in the frequency range determined by the wave gauge spacing, the spectra used to simulate the time series for the laboratory experiments were truncated accordingly. The variance of the full spectra was preserved for the truncated spectra by considering the squared significant wave height ratio given by Eq. (B.6). For the physical simulations performed by Medina et al. (1990), phase spectra resulting in the highest and lowest values for the envelope exceedance coefficient α were chosen for each amplitude spectra. Significant wave heights of consecutive runs were increased in discrete increments such that the stability numbers for the two armor rock sizes were equal in consecutive runs.

APPENDIX A: Rayleigh Distribution

The Rayleigh probability density function (pdf) for the wave amplitudes a (= H/2) is given by

$$p(a) = \frac{a}{\alpha_R^2} \exp\left[-\frac{1}{2}\left[\frac{a}{\alpha_R} \right]^2 \right] U(a) \quad ; \quad \alpha_R > 0 \qquad (A.1a)$$

where α_R = Rayleigh parameter (Hoffman and Karst 1975) and U(a) = Heaviside step function. The Rayleigh cumulative distribution function (cdf) for wave amplitudes is

$$P(a) = 1 - \exp\left[-\frac{1}{2}\left[\frac{a}{\alpha_R} \right]^2 \right] U(a) \quad ; \quad \alpha_R > 0 \qquad (A.1b)$$

The following 4 forms of (A.1a) may be found:

$$p(a) = \frac{\pi a}{2\mu_a^2} \exp\left[-\frac{\pi}{4}\left[\frac{a}{\mu_a} \right]^2 \right] U(a) \quad ; \quad \mu_a > 0 \qquad (A.2a)$$

$$p(H) = \frac{2H}{H_{rms}^2} \exp\left[-\left[\frac{H}{H_{rms}} \right]^2 \right] U(H) \quad ; \quad H_{rms} > 0 \qquad (A.2b)$$

$$p(a) = \frac{a}{m_o} \exp\left[-\frac{1}{2}\left[\frac{a}{\sqrt{m_o}} \right]^2 \right] U(a) \quad ; \quad m_o > 0 \qquad (A.2c)$$

$$p(H) = \frac{H}{4m_o} \exp\left[-\frac{1}{2}\left[\frac{H}{2\sqrt{m_o}} \right]^2 \right] U(H) \quad ; \quad m_o > 0 \qquad (A.2d)$$

where μ_a = average of the amplitude a; H_{rms} = root-mean-square wave height; and m_o =

variance of the time series for the water surface elevation $\eta(t)$. When the random

variable a in (A.2) is scaled by the standard deviation of the time series $\sqrt{m_o}$, then the

following change of variables gives:

$$\xi = \frac{a}{\sqrt{m_o}} \quad ; \quad d\xi = \frac{da}{\sqrt{m_o}}$$

$$p(\xi) = p(a)\frac{da}{d\xi}$$

$$p(\xi) = \frac{a}{\left(\sqrt{m_o}\right)^2} \exp\left[-\frac{a^2}{2m_o}\right]\left(\sqrt{m_o}\right)$$

$$p(\xi) = \xi \exp\left[-\frac{\xi^2}{2}\right] U(\xi) \tag{A.2e}$$

Eqs. (A.2) may be derived from (A.1a) by solving for the generic Rayleigh parameter α_R.

The percent or fraction of wave amplitudes greater than wave amplitude

a_n (= $H_n/2$), may be computed from (A.1a) by

$$n = \int_{a_n}^{\infty} p(a)\,da$$

$$= \exp\left[-\frac{1}{2}\left[\frac{a_n}{\alpha_R}\right]^2\right] \tag{A.3}$$

and the natural logarithm of (A.3) gives

$$\frac{a_n}{\alpha_R} = \sqrt{-2\ln(n)} \qquad (A.4)$$

where $0 < n \le 1$. The average wave amplitude greater than a_n may be determined from

$$\bar{a}_n \int_{a_n}^{\infty} p(a)\,da = \int_{a_n}^{\infty} a\,p(a)\,da$$

that may be integrated by parts to obtain

$$\bar{a}_n(n) = n\,\alpha_R\sqrt{-2\ln(n)} + \int_{a_n}^{\infty} \exp\left[-\frac{1}{2}\left[\frac{a}{\alpha_R}\right]^2\right] da$$

by (A.3) and (A.4). Finally, integration gives

$$\frac{\bar{a}_n}{\alpha_R} = \sqrt{-2\ln(n)} + \frac{1}{n}\sqrt{\frac{\pi}{2}}\left[1 - \mathrm{erf}\left(\sqrt{-\ln(n)}\right)\right] \qquad (A.5a)$$

$$= \sqrt{-2\ln(n)} + \frac{1}{n}\sqrt{\frac{\pi}{2}}\,\mathrm{erfc}\left(\sqrt{-\ln(n)}\right) \qquad (A.5b)$$

where $\mathrm{erf}(\cdot) = $ the error function and $\mathrm{erfc}(\cdot) = $ complementary error function
(Kreyszig 1983). In order to relate the Rayleigh parameter α_R to the average μ_a, set $n = $
1 in Eq. (A.5) and

$$\frac{\bar{a}_n}{\alpha_R} = \frac{\bar{a}_1}{\alpha_R} = \frac{\mu_a}{\alpha_R} = \sqrt{\frac{\pi}{2}}$$

$$\qquad (A.6)$$

$$\alpha_R = \mu_a\sqrt{\frac{2}{\pi}}$$

and substitution into (A.1a) gives (A.2a).

24

Alternatively, (A.5) may be derived directly from special functions according to

$$\bar{a}_n \int_{a_*}^{\infty} p(a)\,da = \int_{a_*}^{\infty} a\,p(a)\,da$$

$$= \alpha_R \left[\sqrt{\frac{\pi}{2}} - \sqrt{2}\,\Gamma\left[\frac{3}{2},0,\frac{a_n^2}{2\alpha_R^2}\right] \right]$$

where the generalized incomplete Gamma function $\Gamma(a,z_0,z_1)$ (Wolfram 1991) is defined

as

$$\Gamma(a,z_0,z_1) = \Gamma(a,z_0) - \Gamma(a,z_1)$$

and the incomplete Gamma function $\Gamma(a,z)$ (Wolfram 1991) is defined as

$$\Gamma(a,z) = \Gamma(a) - G(a,z) = \int_z^{\infty} t^{a-1} \exp(-t)\,dt$$

$$G(a,z) = \int_0^z t^{a-1} \exp(-t)\,dt$$

Substituting for $\Gamma(a,z_0,z_1)$

$$\Gamma\left[\frac{3}{2},0\right] = \frac{\sqrt{\pi}}{2}$$

$$\Gamma\left[\frac{3}{2},\frac{a_n^2}{2\alpha_R^2}\right] = \Gamma\left[\frac{3}{2}\right] - \int_0^{\frac{a_n^2}{2\alpha_R^2}} \sqrt{t}\,\exp(-t)\,dt$$

$$= \int_{\frac{a_n^2}{2\alpha_R^2}}^{\infty} \sqrt{t}\,\exp(-t)\,dt$$

$$= n\sqrt{-\ln(n)} + \frac{\sqrt{\pi}}{2}\left[1 - \mathrm{erf}\left(\sqrt{-\ln(n)}\right)\right]$$

$$= n\sqrt{-\ln(n)} + \frac{\sqrt{\pi}}{2}\,\mathrm{erfc}\left(\sqrt{-\ln(n)}\right)$$

25

giving (A.5).

To relate the Rayleigh parameter α_R to H_{rms}, make the following change of variables in (A.1a):

$$y = a^2 \quad ; \quad dy = 2a\,da = 2\sqrt{y}\,da$$

and

$$p(a)\,da = p(y)\,dy$$

giving

$$p(y) = p(a)\frac{da}{dy}$$

$$= \frac{1}{2\alpha_R^2}\exp\left[-\frac{y}{2\alpha_R^2}\right]U(y)$$

(A.7)

The average of a^2 may now be computed from

$$\overline{a}^2 = a_{rms}^2 = \overline{y} = \int_0^\infty y\,p(y)\,dy$$

$$= \int_0^\infty \frac{y}{2\alpha_R^2}\exp\left[-\frac{y}{2\alpha_R^2}\right]dy$$

(A.8)

$$= 2\alpha_R^2$$

and the Rayleigh parameter α_R may be defined by

$$\alpha_R = \frac{a_{rms}}{\sqrt{2}} = \frac{H_{rms}}{2\sqrt{2}} = \sqrt{m_o} \qquad (A.9)$$

Substituting (A.6) and (A.9) into (A.5b) gives

$$\frac{\bar{a}_n}{\mu_a} = 2\sqrt{-\frac{\ln(n)}{\pi} + \frac{1}{n}\,\mathrm{erfc}\left(\sqrt{-\ln(n)}\right)} \qquad (A.10a)$$

$$\frac{\bar{H}_n}{H_{rms}} = \sqrt{-\ln(n)} + \frac{\sqrt{\pi}}{2n}\,\mathrm{erfc}\left(\sqrt{-\ln(n)}\right) \qquad (A.10b)$$

$$\frac{\bar{H}_n}{\sqrt{m_o}} = \sqrt{-8\ln(n)} + \frac{\sqrt{2\pi}}{n}\,\mathrm{erfc}\left(\sqrt{-\ln(n)}\right) \qquad (A.10c)$$

The significant wave height H_s, or average of the highest 1/3 wave heights $H_{1/3}$ may be computed from (A.5b) for $n = 1/3$ (dropping the overbar average notation) according to

$$\frac{H_{1/3}}{2\alpha_R} = \frac{H_s}{2\alpha_R} = 2.00215 \qquad (A.11a)$$

$$2\alpha_R = \frac{H_s(H_{1/3})}{2.00215} \qquad (A.11b)$$

Substituting (A.11b) into (A.5b) gives

27

$$\frac{\bar{H}_n}{H_s\left(H_{1/3}\right)} = (2.00215)^{-1}\left\{\sqrt{-2\ln(n)} + \frac{1}{n}\sqrt{\frac{\pi}{2}}\ \text{erfc}\left(\sqrt{-\ln(n)}\right)\right\} \qquad (A.12)$$

To find the mode (or most probable) value of a_{mode} ($= H_{mode}/2$), the maximum value of (A.1a) occurs when

$$\frac{dp(a)}{da} = 0 \quad ; \quad a = a_{mode} \qquad (A.13)$$

giving

$$a_{mode} = \alpha_R \quad ; \quad H_{mode} = 2\alpha_R \qquad (A.14a,b)$$

and

$$\frac{a_{mode}}{\mu_a} = \sqrt{\frac{2}{\pi}} \quad ; \quad \frac{H_{mode}}{H_{rms}} = \frac{1}{\sqrt{2}} \qquad (A.15a,b)$$

$$\frac{H_{mode}}{\sqrt{m_o}} = 2 \quad ; \quad \frac{H_{mode}}{H_s\left(H_{1/3}\right)} = (2.00215)^{-1} \qquad (A.15c,d)$$

The mean or median of a occurs when $P(a) = 0.5$ in (A.1b). The natural logarithm of (A.1b) for $P(a_{med}) = 0.5$ is

$$\frac{a_{med}}{\alpha_R} = \sqrt{2\ln(2)} \qquad (A.16)$$

28

giving

$$\frac{a_{med}}{\mu_a} = \sqrt{\frac{4\ln(2)}{\pi}} \quad ; \quad \frac{H_{med}}{H_{rms}} = \sqrt{\ln(2)} \qquad \text{(A.17a,b)}$$

$$\frac{H_{med}}{\sqrt{m_o}} = \sqrt{8\ln(2)} \quad ; \quad \frac{H_{med}}{H_s(H_{1/3})} = \frac{\sqrt{2\ln(2)}}{2.0015} \qquad \text{(A.17c,d)}$$

These results are summarized in Table A.1

height	$\dfrac{H}{\mu_a}$	$\dfrac{H}{H_{rms}}$	$\dfrac{H}{\sqrt{m_o}}$	$\dfrac{H}{H_s(H_{1/3})}$
H_{mode}	$\sqrt{\dfrac{8}{\pi}}$	$\dfrac{1}{\sqrt{2}}$	2.0	$(2.00215)^{-1}$
$H_{med}(P=1/2)$	$4\sqrt{\dfrac{\ln(2)}{\pi}}$	$\sqrt{\ln(2)}$	$\sqrt{8\ln(2)}$	$\dfrac{\sqrt{2\ln(2)}}{2.00215}$
$H_1(=\text{mean})$	2.0	$\dfrac{\sqrt{\pi}}{2}$	$\sqrt{2\pi}$	$\dfrac{\sqrt{\pi/2}}{2.00215}$
$H_s(H_{1/3})$	3.19497	1.41573	4.0043	1.0
$H_{1/10}$	4.06198	1.79992	5.09094	1.27137
$H_{1/100}$	5.32423	2.35924	6.67293	1.66644

Table A.1 - Rayleigh distributed wave height relationships

APPENDIX B: Simulation of Sea States

In order to correctly describe wave groups in laboratory studies, the incident wave train must be known. An algorithm developed at Oregon State University by Fassardi (1993) was used to resolve the incident and reflected wave trains in a finite bandwidth determined by the wave gauge spacing $\Delta \ell$ (Table 3.1). One broad ($\gamma=1$) and one narrow ($\gamma=10$) truncated Goda-JONSWAP spectrum (Goda 1985) were simulated according to

$$S_\eta(f) = c_1 H_R H_{s,trunc}^2 \frac{f_p^4}{f^5} \exp[-1.25(\frac{f}{f_p})^{-4}]\gamma^{\exp[-(\frac{f}{f_p}-1)^2/2\sigma^2]} \tag{B.1}$$

$$c_1 = \frac{0.0624}{0.230 + 0.0336\gamma - 0.185(1.9 + \gamma)^{-1}} \tag{B.2}$$

$$\sigma = \begin{cases} 0.07 : f \le f_p \\ 0.09 : f \ge f_p \end{cases} \tag{B.3}$$

for $f_{min} \le f \le f_{max}$, where f_p is the peak frequency, H_R is the squared significant wave height ratio defined in Eq. (B.6), and $H_{s,trunc}$ is the significant wave height of the truncated spectrum. Eq. (B.1) is different than Eq. (30) in Fassardi (1993) in that Fassardi (1993) does not document the use of the constant c_1 defined by Eq. (B.2). The spectra were truncated according to

$$f_{min} = 0.7f_p$$
$$f_{max} = 2.5f_p \tag{B.4}$$

To define the truncated spectra and preserve the variance of the full spectra, Eq. (B.1) includes the dimensionless coefficient H_R. If the significant wave height is given in terms of the variance (Table A.1) by

$$H_s = 4.0043\sqrt{m_0} \qquad (B.5)$$

then the squared significant wave height ratio H_R may be defined as

$$H_R = \frac{H_{s,full}^2}{H_{s,trunc}^2} \qquad (B.6)$$

where $H_{s,full}$ is the significant wave height of the full spectra. For peak frequencies between 0.1 and 0.5 Hz, the average dimensionless variance preserving coefficients for $\gamma = 1$ and $\gamma = 10$ are $H_R = 1.0375$ and $H_R = 1.0133$ respectively.

The mean frequency of the truncated spectra defined by the first and zeroeth spectral moments

$$\bar{f} = \frac{m_1}{m_0} \qquad (B.7)$$

was held constant at $\bar{f} = 0.3333$ Hz such that the peak frequency of the truncated spectra could be computed from the frequency ratio

$$f_R = \frac{f_p}{\bar{f}} \qquad (B.8)$$

For peak frequencies between 0.1 and 0.5 Hz, the average frequency ratios were

31

$f_R = 0.8115$ and $f_R = 0.9173$ for $\gamma = 1$ and $\gamma = 10$, respectively. Accordingly, the peak frequencies used to simulate the truncated spectra from Eq. (B.1) were $f_p = 0.2705$ Hz and $f_p = 0.3058$ Hz for $\gamma = 1$ and $\gamma = 10$, respectively.

The wave gauge spacing defined by Figure 3.1 was 1.22m, and the water depth was 3.05m (Fassardi 1993). If the band pass filter limits proposed by Goda and Suzuki (1976) given by Eq. (3.6a) are used, and the linear wave theory dispersion relationship is given by

$$\omega = \sqrt{ g \frac{2\pi}{L} \tanh \frac{2\pi h}{L} } \quad ; \qquad\qquad (B.9)$$

the minimum and maximum resolvable frequencies for $\Delta \ell = 1.22$m are $f_{min} = 0.1299$ Hz and $f_{max} = 0.7589$ Hz. For cases where $\gamma = 1$, the minimum and maximum frequencies of the truncated spectra are $f_{min} = 0.1894$ Hz and $f_{max} = 0.6762$ Hz. For $\gamma = 10$, the minimum and maximum frequencies of the truncated spectra are $f_{min} = 0.2140$ Hz and $f_{max} = 0.7644$ Hz. These frequency limits for the truncated spectra are reasonably close to those resolvable by wave gauges spatially separated by $\Delta \ell = 1.22$m.

Different phase spectra produce time series with different wave grouping characteristics. Accordingly, time series were synthesized using two different phase spectra for each of the truncated Goda-JONSWAP spectra given by Eq. (B.1) with $\gamma = 1, 10$ and $\bar{f} = 0.3333$ Hz. The phase spectra were chosen from 100 random Deterministic Spectral Amplitude (DSA) simulations for each amplitude spectra. Values of α were calculated from each DSA simulated time series according to Eq. (2.5). For

each γ, the phase spectra that produced the wave envelope $A(x,t)$ with the highest and lowest wave height variability characterized by α were chosen for the physical simulations. The parameters used for wave simulation are summarized in Table B.1.

γ	c_1	H_R	f_R	f_p	resolvable for $\Delta\ell=1.22$m from Eq. (3.6a)		f_{min}	f_{max}	Low α from DSA	High α from DSA
					f_{min}	f_{max}				
1	0.3123	1.0375	0.8115	0.2705	0.1299	0.7589	0.1894	0.6762	0.51	2.18
10	0.1134	1.0133	0.9173	0.3058	0.1299	0.7589	0.2140	0.7644	0.23	2.52

Table B.1 - Summary of simulation parameters for $\Delta\ell=1.22$m and h$=3.05$m
(frequencies in Hz)

Realizations with the same envelope, but different phase-shifted wave profiles are given by (Medina et al. 1994)

$$\eta_\phi(x,t)=\sum_{m=1}^{M} a_m \cos[kx-\omega t-(\varepsilon+\phi)] \tag{B.10}$$

where ϕ is a constant phase shift applied to all M wave components. Three different phase shifted realizations ($\phi=0, 2\pi/3, 4\pi/3$) and the replicate ($\phi=2\pi$) for each of the four wave envelopes were tested to determine if realizations shifted by a constant phase produce different levels of damage. For each γ, $A(x,t)$, and constant phase shift ϕ, a sequence of time series were tested with increasing significant wave heights.

The breakwater model tested by Medina et al. (1990) was divided in the direction of wave propagation into two sides with a different armor layer rock size (viz., $W_L = 128.5$ N and $W_s = 99.1$ N) on each side. The monochromatic wave height corresponding to the zero damage condition (SPM 1984) can be calculated from

$$H = \left[\frac{W K_D \left(\frac{\rho_r}{\rho_w} - 1 \right)^3 \cot\Theta}{\rho_r} \right]^{\frac{1}{3}} \tag{B.11}$$

where W is the median value of the mass distribution of rocks in the armor; K_D is the stability coefficient; Θ is the angle of the breakwater slope measured from horizontal, and ρ_r and ρ_w are the weight densities of the rocks and water, respectively. Solving Eq. (B.11) numerically for the small rock size ($W_s = 99.1$ N) yields a monochromatic wave height of H=0.55m for the zero damage condition. Breakwater model and armor rock characteristics are given in Table B.2.

W_L (N)	W_s (N)	K_D	ρ_r (kN/m^3)	ρ_w (kN/m^3)	$\cot\Theta$
128.5	99.1	4	27.4	9.8	2

Table B.2 - Summary of breakwater model characteristics (Fassardi 1993)

For the zero damage condition, if the representative design wave height for a random sea is $H_{1/10}$, then the design significant wave height for the small rock size is determined (Table A.1) by

34

$$H_s = \frac{0.55m}{1.27137} = 0.43m \text{ for } W_s = 99.1 \text{ N} \qquad (B.12)$$

An empirically derived number which controls the stability of the armor layer (Medina et al. 1990) is given by

$$N_s = \left[\frac{\rho_r H_s^3}{W \left(\frac{\rho_r}{\rho_w} - 1 \right)^3} \right]^{\frac{1}{3}} \qquad (B.13)$$

where N_s is the stability number, and H_s is the design significant wave height. The significant wave heights in the physical simulations were increased in discrete increments such that the stability numbers given by Eq. (B.13) for the large (W_L) and small (W_S) rocks were equal in consecutive runs. Seven significant wave heights were tested for each of the sixteen realizations. The significant wave heights varied from the design significant wave height of the small rock size to the maximum wave height, avoiding breaking. From Eq. (B.13), the significant wave height of the kth run is given by

$$H_{s,(k)} = 0.43 \left[\frac{W_L}{W_S} \right]^{\frac{k-1}{3}} \quad ; \quad k = 1, 2, \ldots, 7 \qquad (B.14)$$

Thus, twenty-eight realizations of four phases and seven wave heights were simulated for each of four target envelopes shown in Figure B.1. For each realization, runs of approximately 30 minutes long containing $N = 2^{15} = 32768$ points sampled at $\Delta t = 0.06$ seconds were simulated.
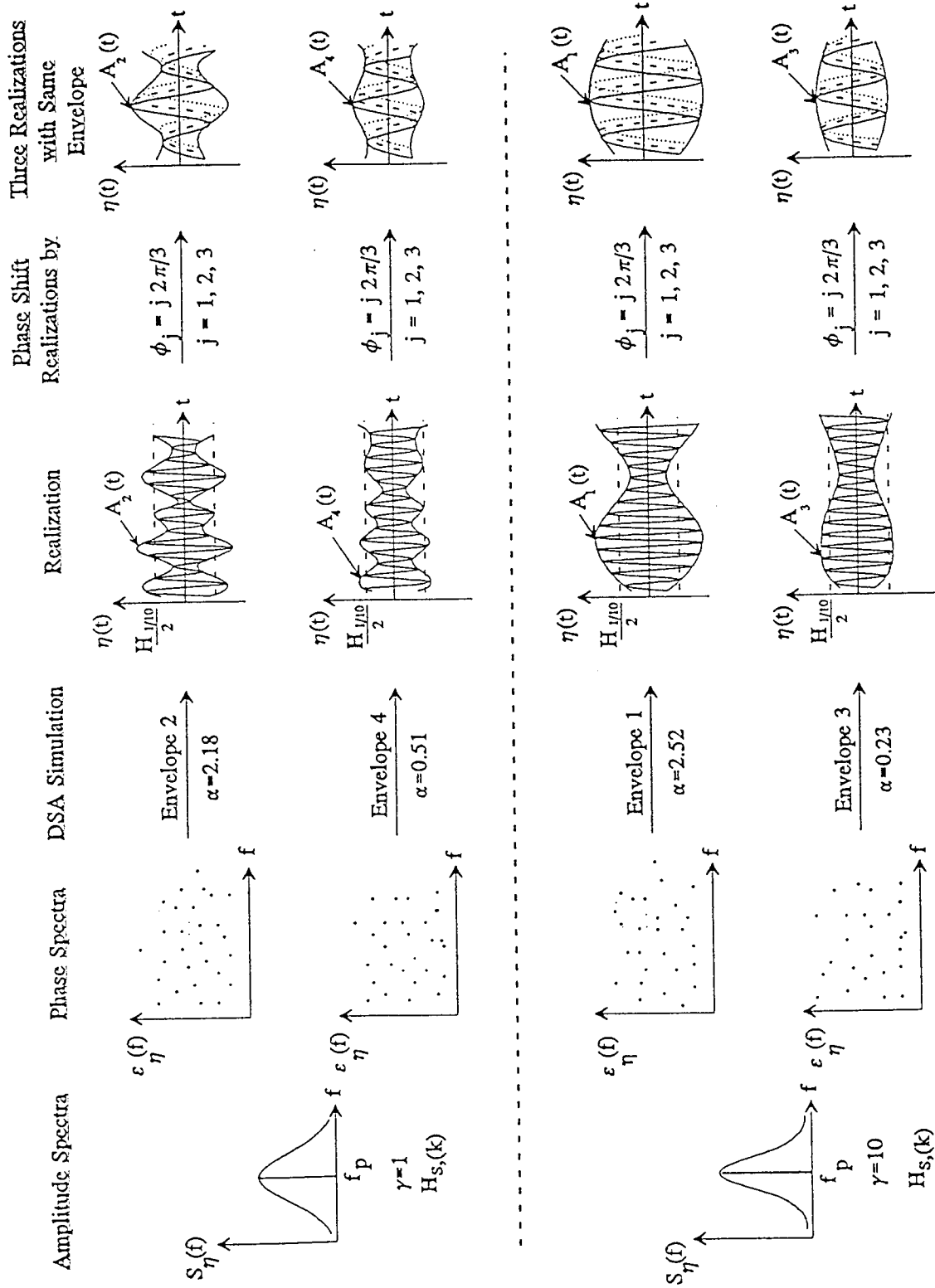
Figure B.1 - Simulation of Realizations with Wave Height $H_{s(k)}$

APPENDIX C: Wave Time Series and Spectra

37

RESOLVING INCIDENT AND REFLECTED TRAINS FOR RECORD: elp1l7

Gauge No. : 1
  Raw Time Series Mean Value : 0.009327   Variance :   0.040746

Gauge No. : 2
  Raw Time Series Mean Value : 0.010709   Variance :   0.038375

Gauge No. : 3
  Raw Time Series Mean Value : 0.006861   Variance :   0.036691

RESOLVED INCIDENT AND REFLECTED WAVES

Analysis from Gauges 2 and 3

  Incident wave Spectrum's Variance: 0.032890
  Reflected wave Spectrum's Variance: 0.001678

  Breakwater's reflection coefficient : 0.2259
  Incident significant wave height : 0.7261
  Reflected significant wave height : 0.1640
  Mean Period (T01) from incident spectrum : 3.065

  Incident wave train, Mean and Variance from TS(2,3)
    TS Mean : 0.000000 TS Variance : 0.032890

  Reflected wave train, Mean and Variance from TS(2,3)
   TS Mean : 0.000000 TS Variance : 0.001678

Analysis from Gauges 1 and 2

  Incident wave Spectrum's Variance: 0.033244
  Reflected wave Spectrum's Variance: 0.002225

  Breakwater's reflection coefficient : 0.2587
  Incident significant wave height : 0.7300
  Reflected significant wave height : 0.1889
  Mean Period (T01) from incident spectrum : 3.074

  Incident wave train, Mean and Variance from TS(1,2)
    TS Mean : 0.000000 TS Variance : 0.033244

  Reflected wave train, Mean and Variance from TS(1,2)
    TS Mean : 0.000000 TS Variance : 0.002225
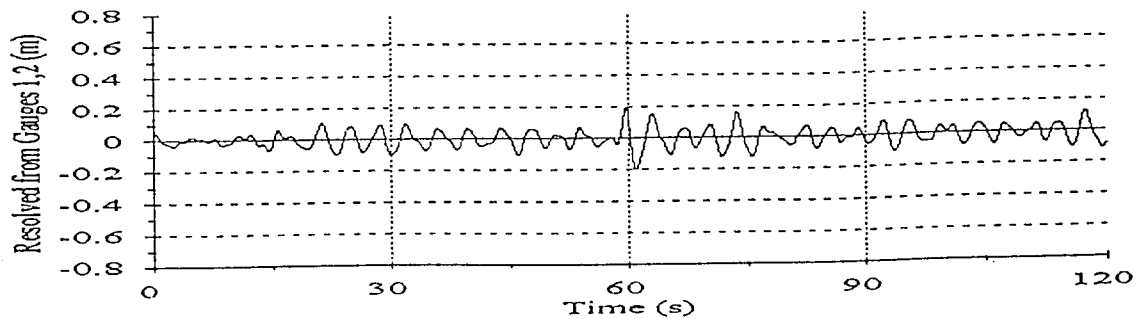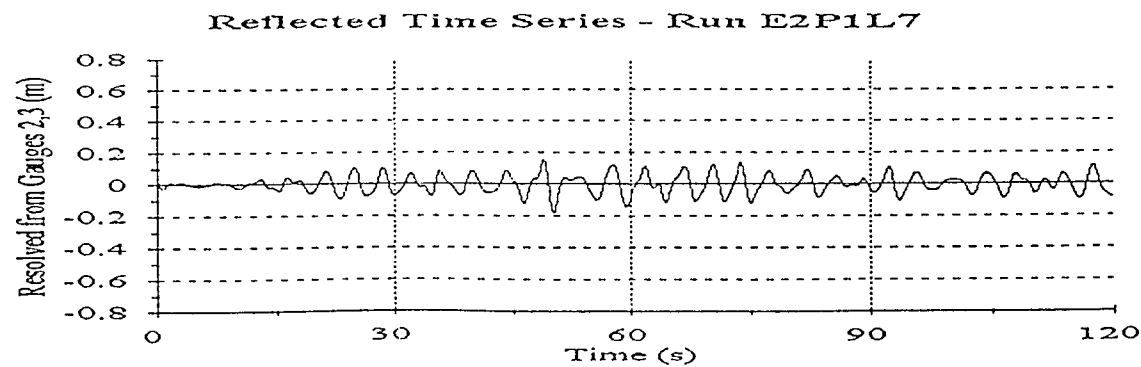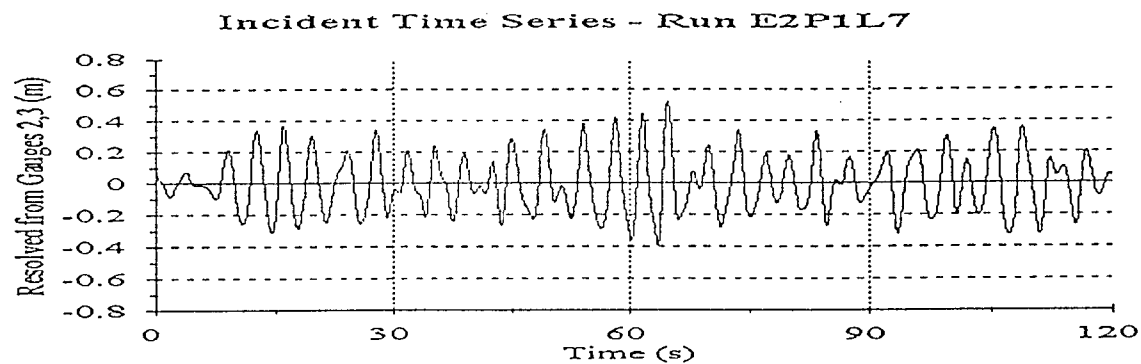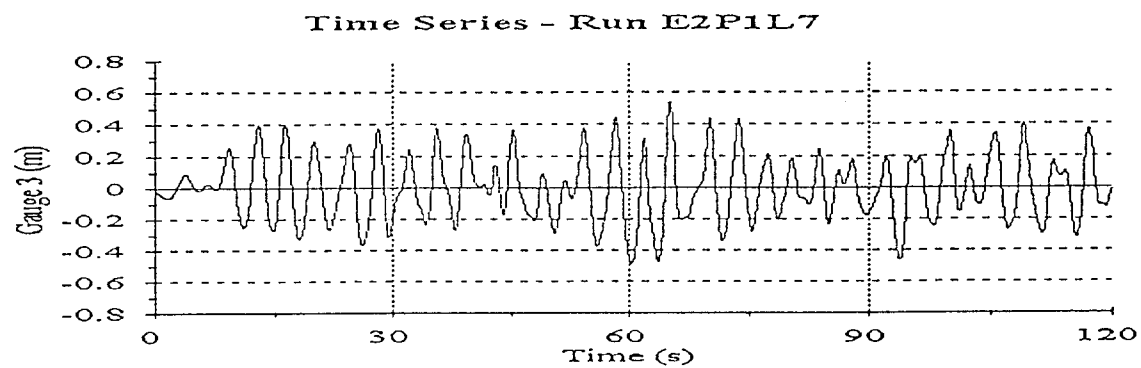
Time Series – Run E1P1L7

Time Series – Run E1P1L7

Incident Time Series – Run E1P1L7

Reflected Time Series – Run E1P1L7

39
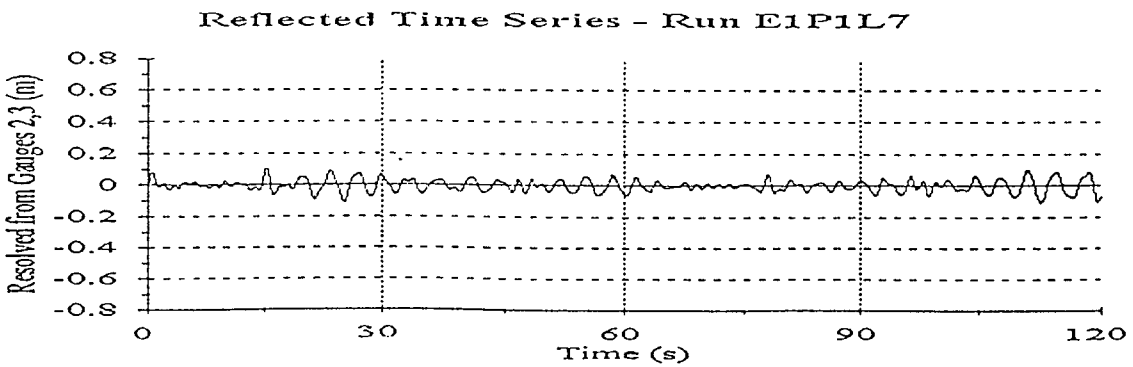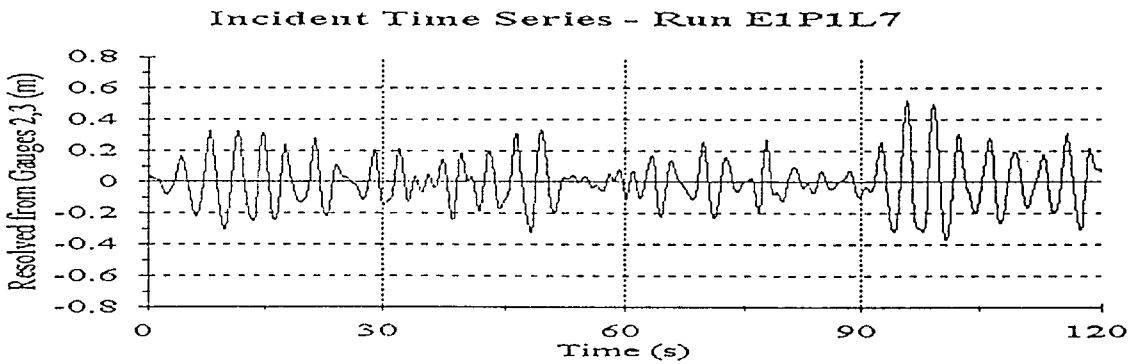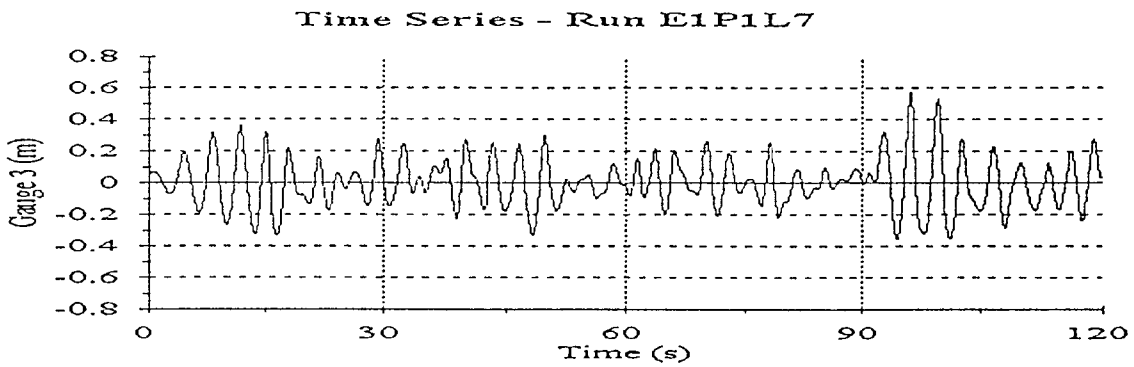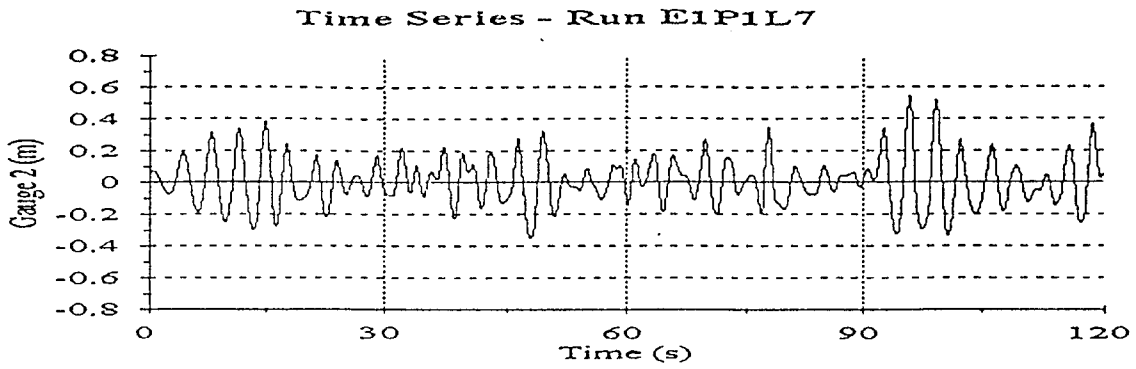
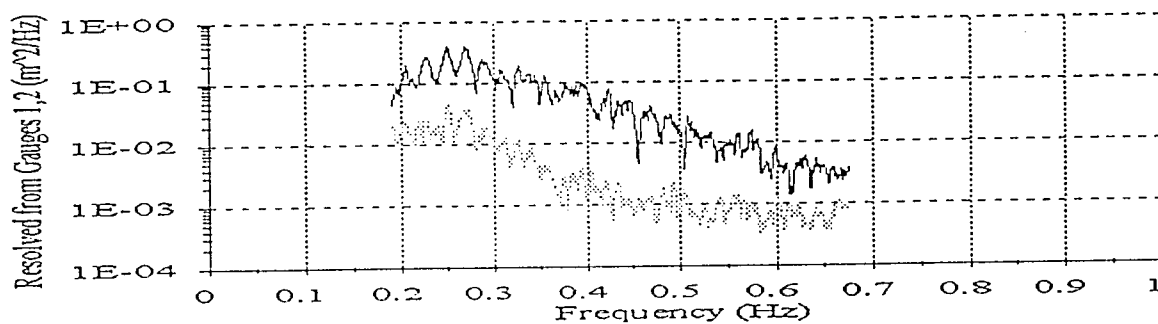# RESOLVING INCIDENT AND REFLECTED TRAINS FOR RECORD: e2p1l7

Gauge No. : 1
  Raw Time Series Mean Value : 0.009919   Variance :   0.039530

Gauge No. : 2
  Raw Time Series Mean Value : 0.003559   Variance :   0.041591

Gauge No. : 3
  Raw Time Series Mean Value : -0.010094   Variance :   0.041708

RESOLVED INCIDENT AND REFLECTED WAVES

Analysis from Gauges 2 and 3

  Incident wave Spectrum's Variance: 0.031342
  Reflected wave Spectrum's Variance: 0.002484

  Breakwater's reflection coefficient : 0.2815
  Incident significant wave height : 0.7089
  Reflected significant wave height : 0.1996
  Mean Period (T01) from incident spectrum : 3.245

  Incident wave train, Mean and Variance from TS(2,3)
    TS Mean : 0.000000 TS Variance : 0.031342

  Reflected wave train, Mean and Variance from TS(2,3)
    TS Mean : 0.000000 TS Variance : 0.002484

Analysis from Gauges 1 and 2

  Incident wave Spectrum's Variance: 0.033780
  Reflected wave Spectrum's Variance: 0.002935

  Breakwater's reflection coefficient : 0.2948
  Incident significant wave height : 0.7359
  Reflected significant wave height : 0.2169
  Mean Period (T01) from incident spectrum : 3.244

  Incident wave train, Mean and Variance from TS(1,2)
    TS Mean : 0.000000 TS Variance : 0.033780

  Reflected wave train, Mean and Variance from TS(1,2)
    TS Mean : 0.000000 TS Variance : 0.002935

Time Series – Run E2P1L7

Time Series – Run E2P1L7

Incident Time Series – Run E2P1L7

Reflected Time Series – Run E2P1L7

41

Time Series – Run E2P1L7
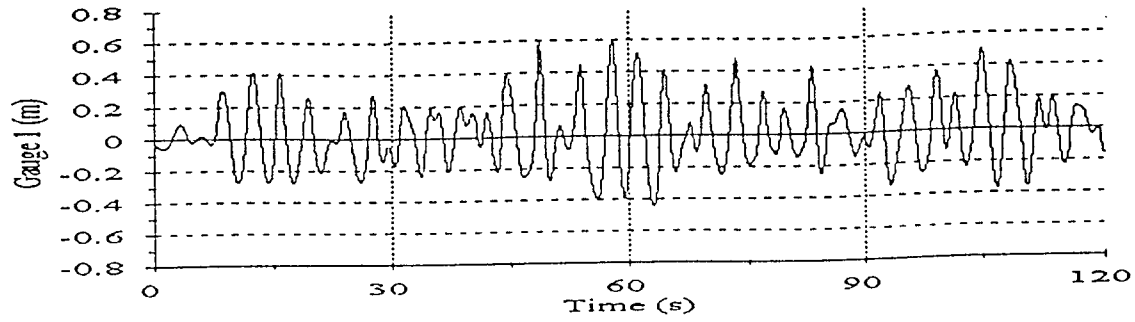
Time Series – Run E2P1L7
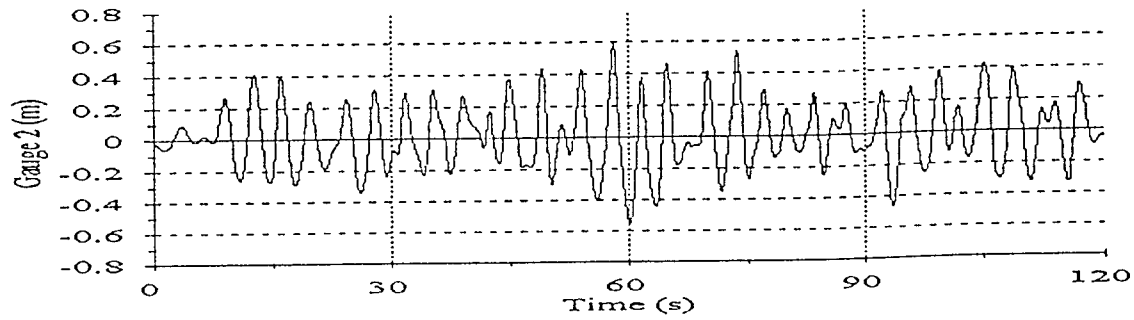
Incident Time Series – Run E2P1L7
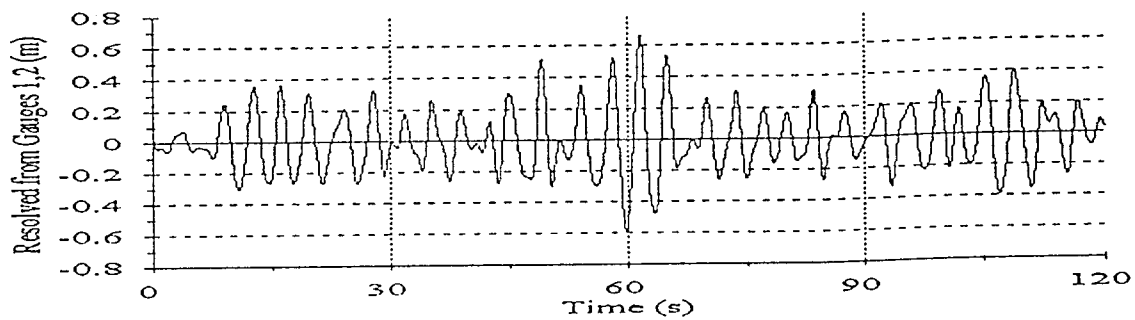
Reflected Time Series – Run E2P1L7
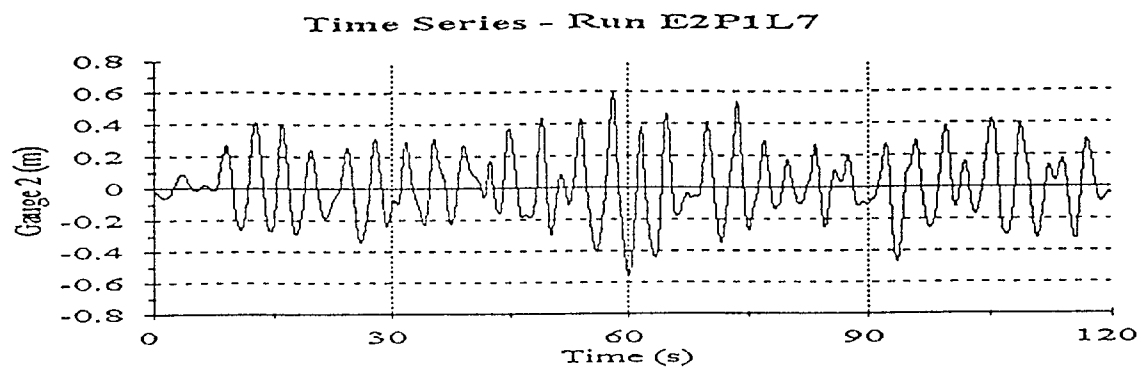
Composite Spectrum – Run E2P1L7
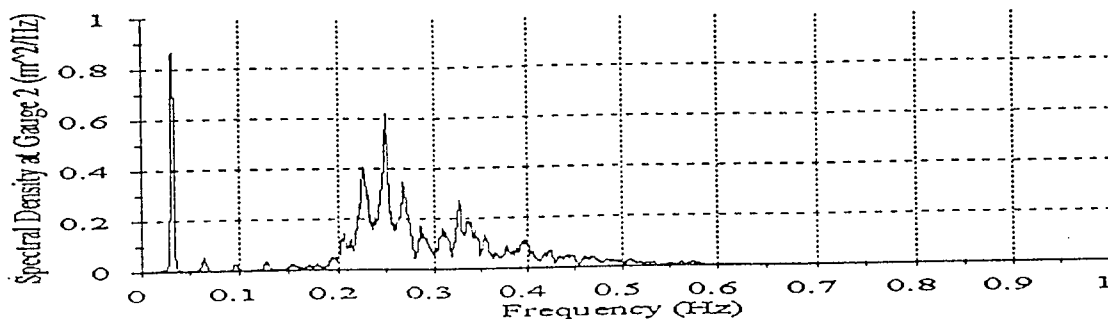
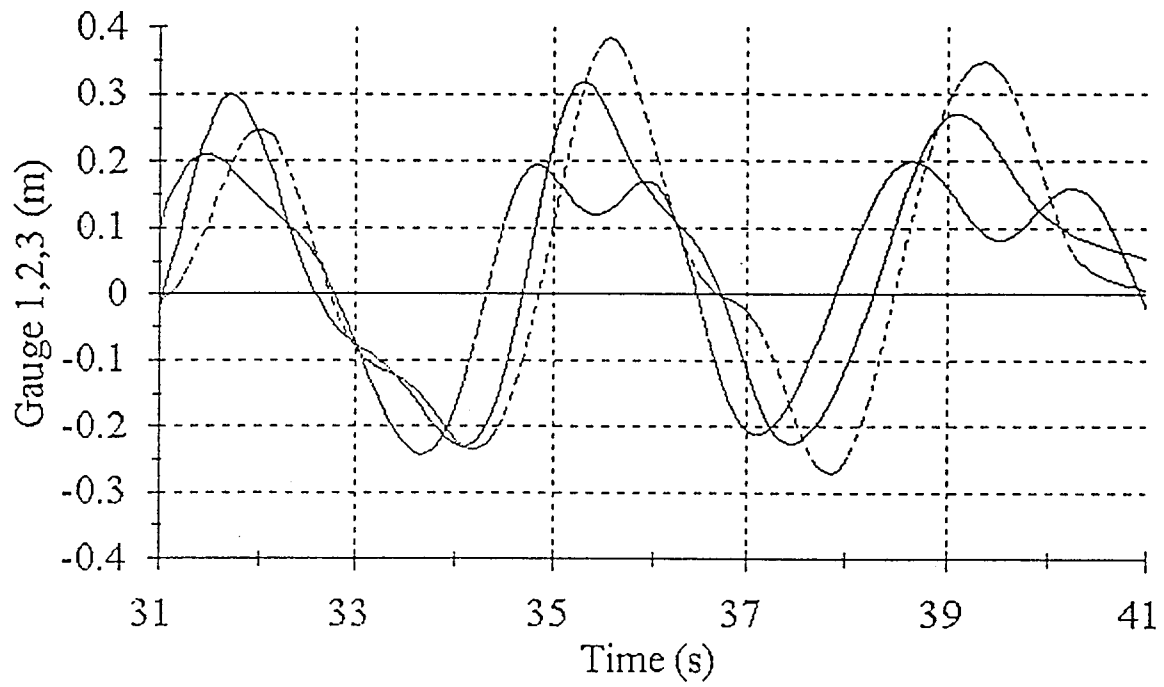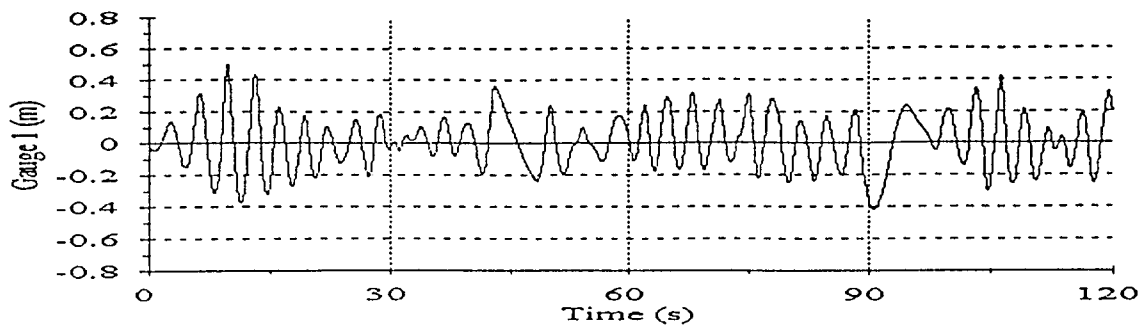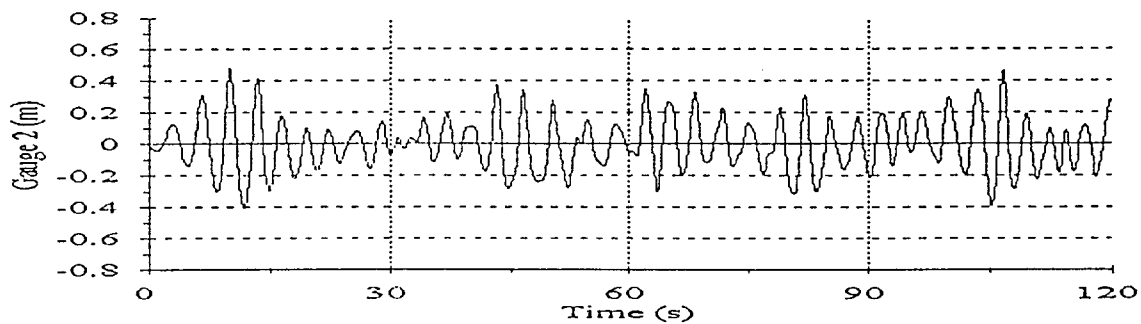Composite Spectrum – Run E2P1L7
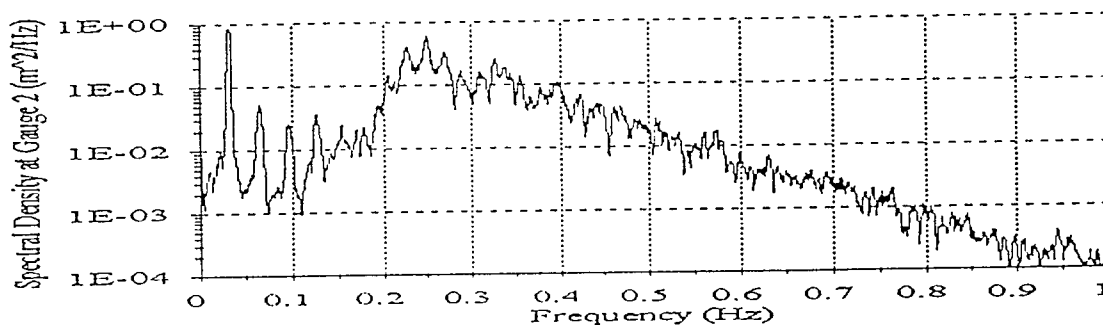
Inc. and Ref. Spectra – Run E2P1L7

INCIDENT   REFLECTED

Inc. and Ref. Spectra – Run E2P1L7
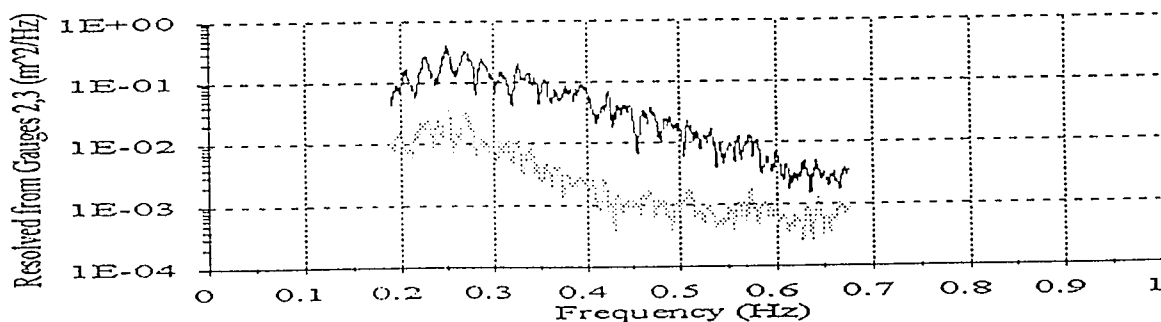
INCIDENT   REFLECTED

Time Series - Run E2P1L7

- · GAUGE 1 —— GAUGE 2 --- GAUGE 3

RESOLVING INCIDENT AND REFLECTED TRAINS FOR RECORD: e3p1l7

Gauge No. : 1
  Raw Time Series Mean Value : 0.011743   Variance :   0.041173

Gauge No. : 2
  Raw Time Series Mean Value : 0.002714   Variance :   0.038172

Gauge No. : 3
  Raw Time Series Mean Value : -0.002450   Variance :   0.038333

RESOLVED INCIDENT AND REFLECTED WAVES

Analysis from Gauges 2 and 3

  Incident wave Spectrum's Variance: 0.035032
  Reflected wave Spectrum's Variance: 0.001793

  Breakwater's reflection coefficient : 0.2262
  Incident significant wave height : 0.7494
  Reflected significant wave height : 0.1695
  Mean Period (T01) from incident spectrum : 3.056

  Incident wave train, Mean and Variance from TS(2,3)
    TS Mean :   0.000000 TS Variance :   0.035032

  Reflected wave train, Mean and Variance from TS(2,3)
    TS Mean :   0.000000 TS Variance :   0.001793

Analysis from Gauges 1 and 2

  Incident wave Spectrum's Variance: 0.034591
  Reflected wave Spectrum's Variance: 0.002552

  Breakwater's reflection coefficient : 0.2716
  Incident significant wave height : 0.7447
  Reflected significant wave height : 0.2023
  Mean Period (T01) from incident spectrum : 3.078

  Incident wave train, Mean and Variance from TS(1,2)
    TS Mean :   0.000000 TS Variance :   0.034591

  Reflected wave train, Mean and Variance from TS(1,2)
    TS Mean :   0.000000 TS Variance :   0.002552
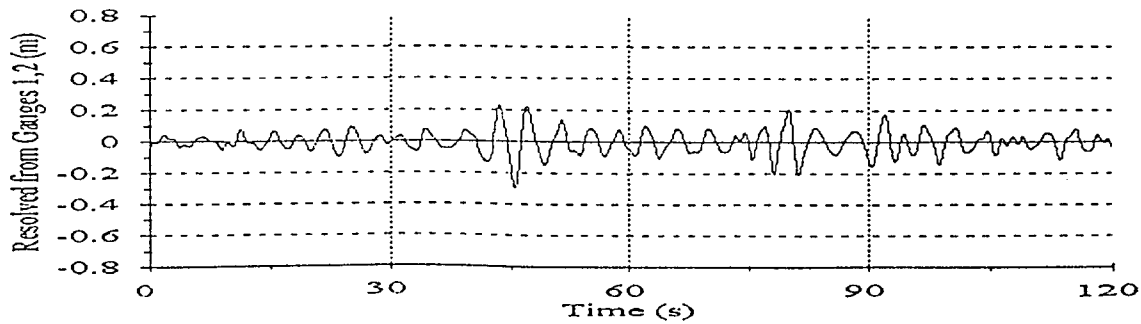
45

Time Series - Run E3P1L7
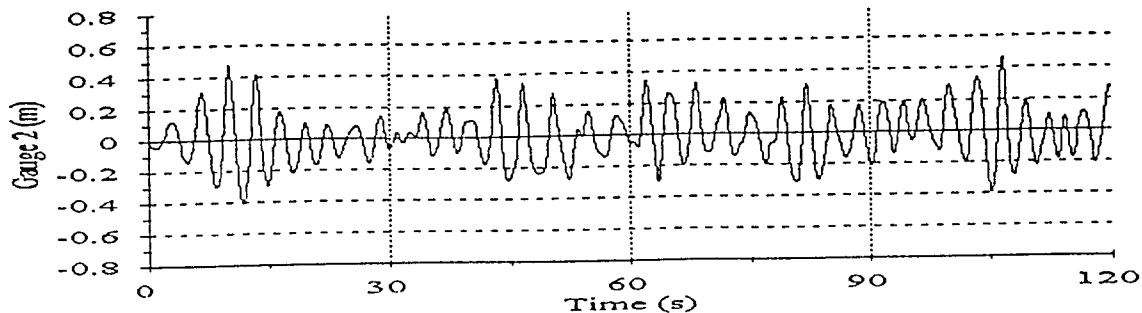

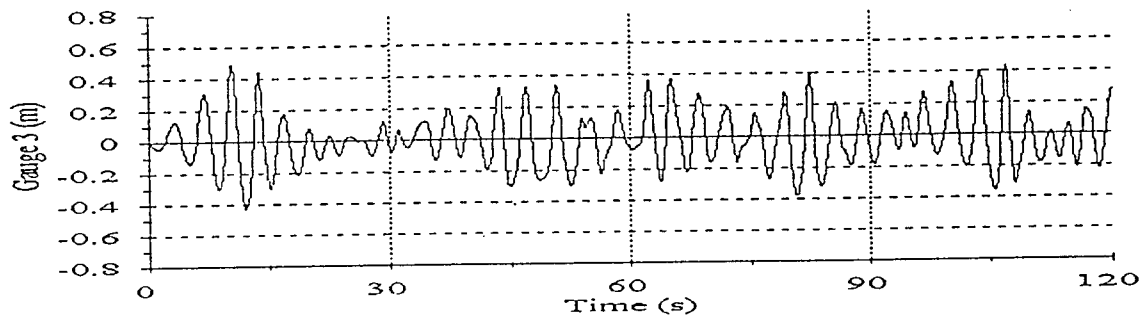## Time Series - Run E3P1L7

Incident Time Series - Run E3P1L7
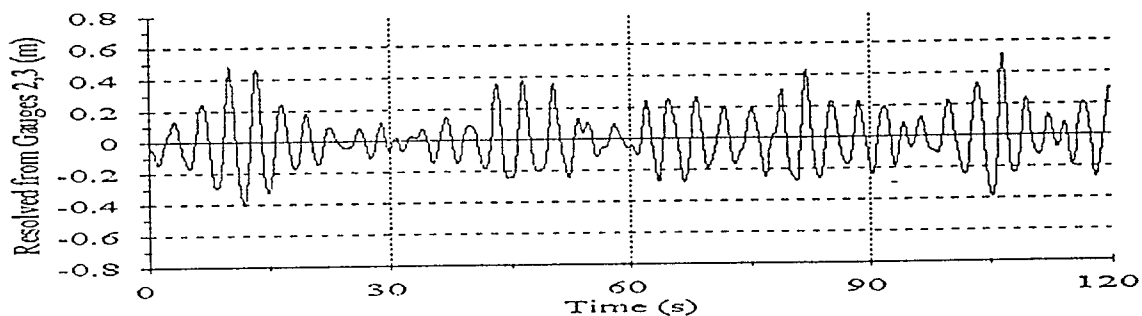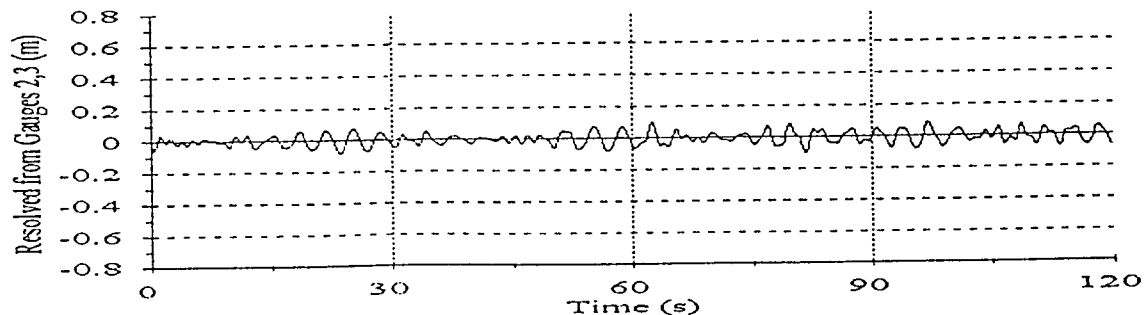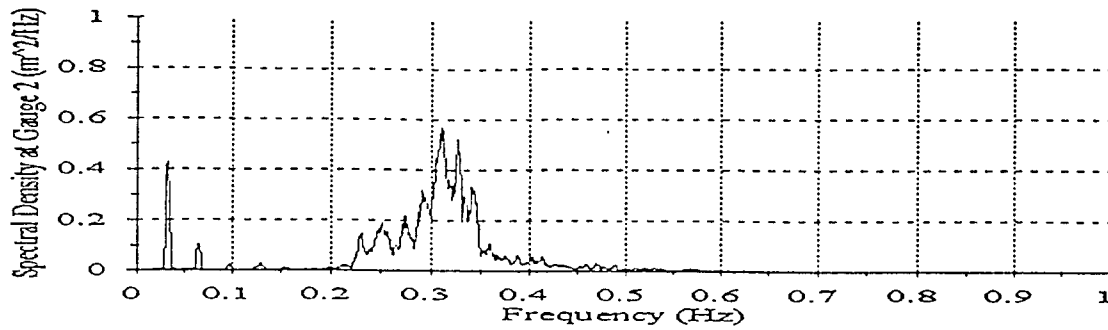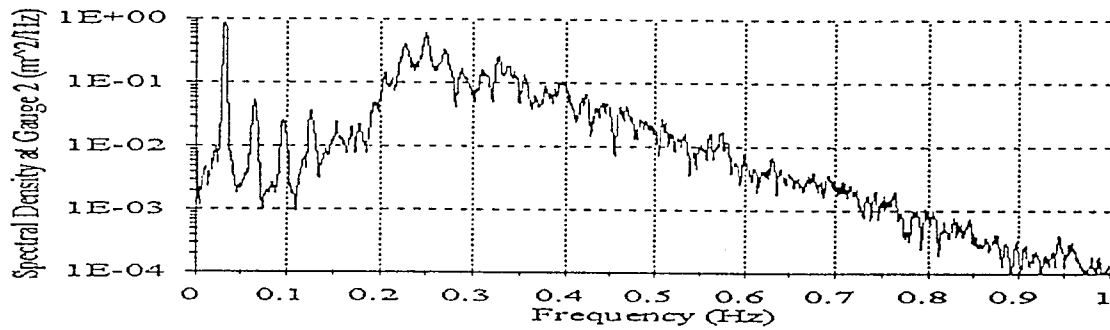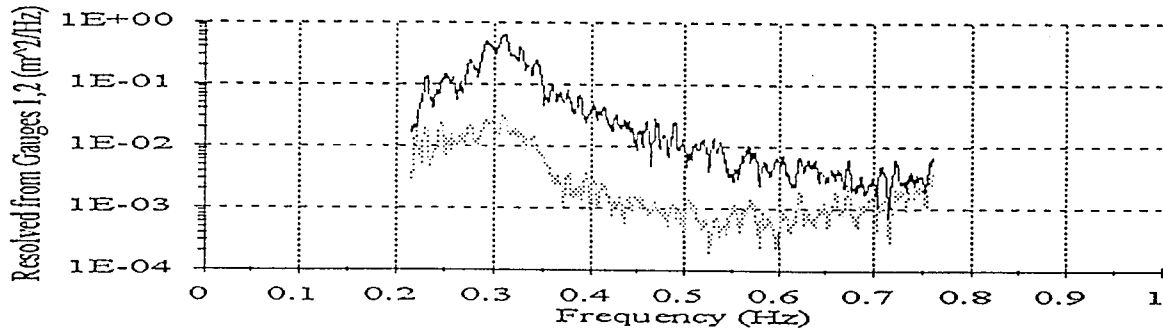

Reflected Time Series - Run E3P1L7

46
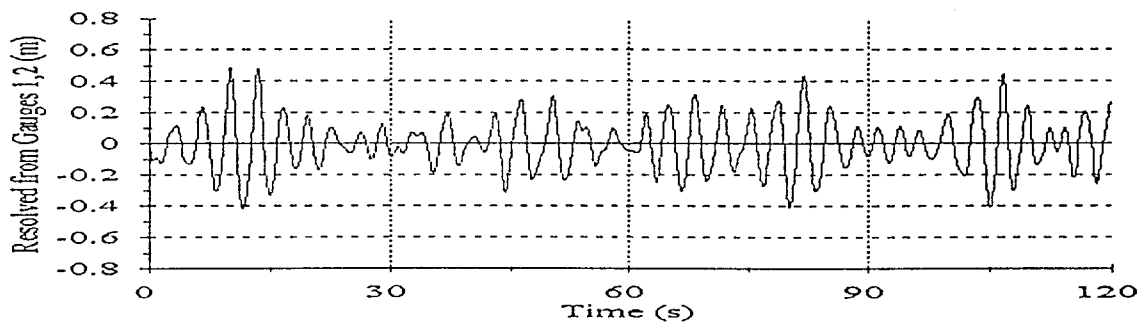
Time Series – Run E3P1L7

Time Series – Run E3P1L7

Incident Time Series – Run E3P1L7

Reflected Time Series – Run E3P1L7

Composite Spectrum – Run E3P1L7

Spectral Density at Gauge 2 (m^2/Hz) vs Frequency (Hz)

Composite Spectrum – Run E2P1L7

Spectral Density at Gauge 2 (m^2/Hz) vs Frequency (Hz)

Inc. and Ref. Spectra – Run E3P1L7

Resolved from Gauges 1,2 (m^2/Hz) vs Frequency (Hz)

INCIDENT   REFLECTED

Inc. and Ref. Spectra – Run E3P1L7

Resolved from Gauges 2,3 (m^2/Hz) vs Frequency (Hz)

INCIDENT   REFLECTED

48

Time Series - Run E3P1L7

RESOLVING INCIDENT AND REFLECTED TRAINS FOR RECORD: e4p117

Gauge No. : 1
   Raw Time Series Mean Value : 0.015713   Variance :   0.043060

Gauge No. : 2
   Raw Time Series Mean Value : 0.025821   Variance :   0.041359

Gauge No. : 3
   Raw Time Series Mean Value : 0.029771   Variance :   0.044257

RESOLVED INCIDENT AND REFLECTED WAVES

Analysis from Gauges 2 and 3

  Incident wave Spectrum's Variance: 0.036691
  Reflected wave Spectrum's Variance: 0.002226

  Breakwater's reflection coefficient : 0.2463
  Incident significant wave height : 0.7670
  Reflected significant wave height : 0.1889
  Mean Period (T01) from incident spectrum : 3.206

  Incident wave train, Mean and Variance from TS(2,3)
    TS Mean : 0.000000 TS Variance : 0.036691

  Reflected wave train, Mean and Variance from TS(2,3)
    TS Mean : 0.000000 TS Variance : 0.002226

Analysis from Gauges 1 and 2

  Incident wave Spectrum's Variance: 0.036596
  Reflected wave Spectrum's Variance: 0.002472

  Breakwater's reflection coefficient : 0.2599
  Incident significant wave height : 0.7660
  Reflected significant wave height : 0.1991
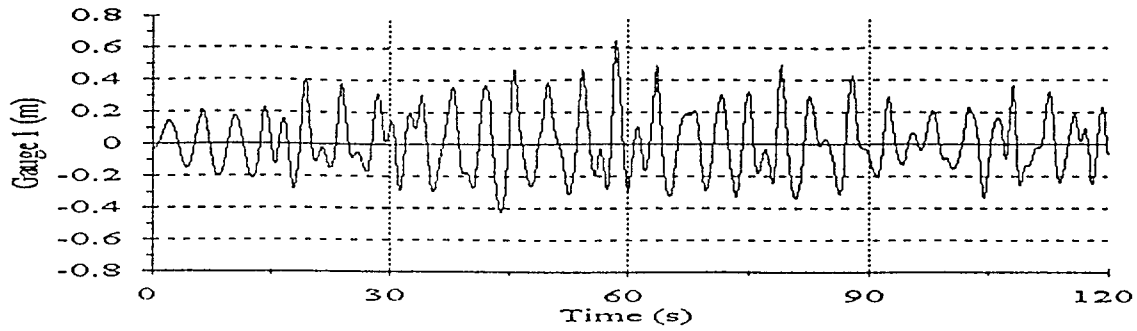 Mean Period (T01) from incident spectrum : 3.212

  Incident wave train, Mean and Variance from TS(1,2)
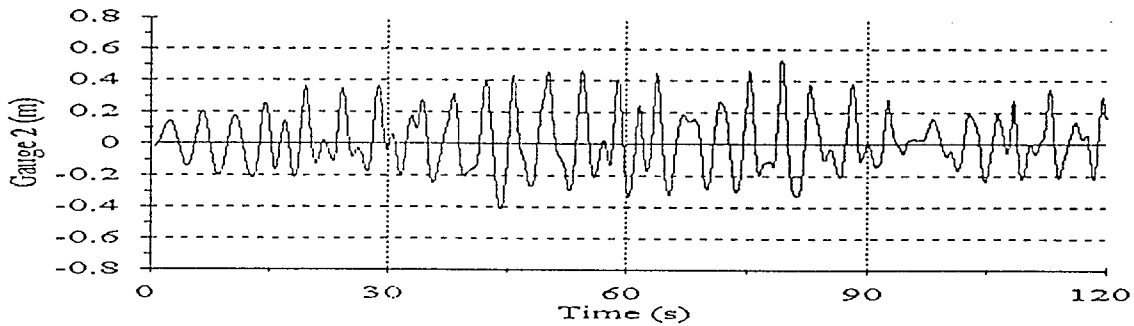   TS Mean : 0.000000 TS Variance : 0.036595

  Reflected wave train, Mean and Variance from TS(1,2)
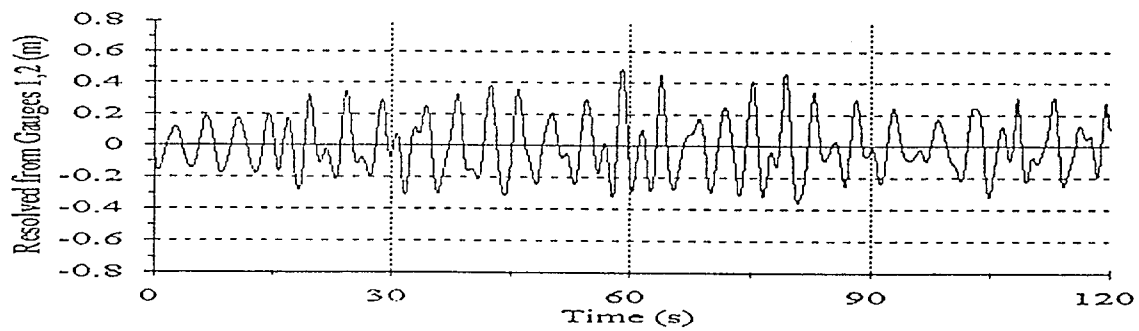   TS Mean : 0.000000 TS Variance : 0.002472
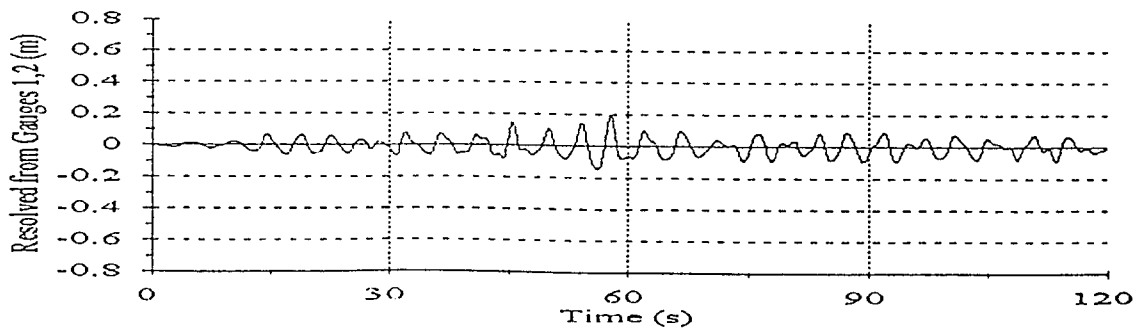
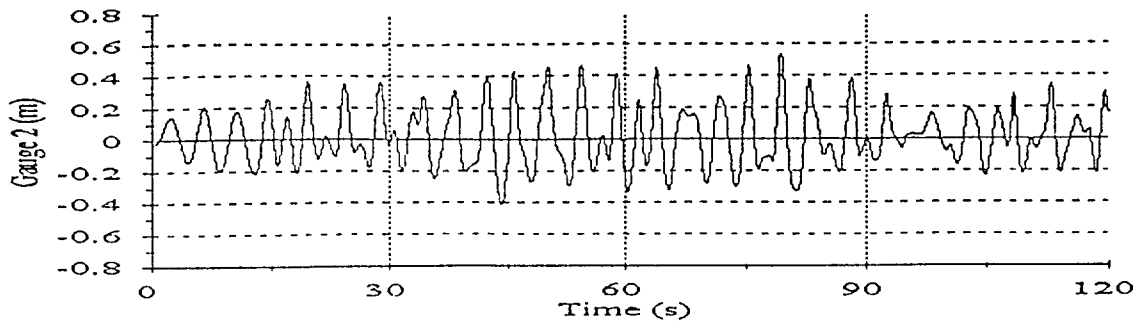## Time Series – Run E4P1L7

Time Series – Run E4P1L7

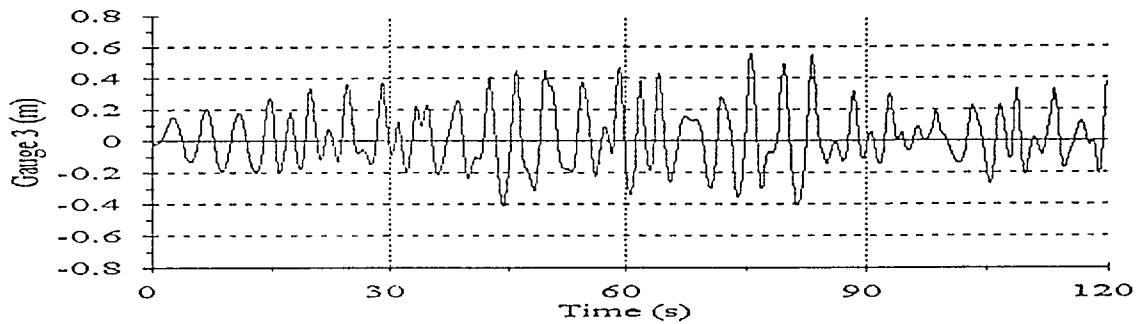## Incident Time Series – Run E4P1L7

Reflected Time Series – Run E4P1L7

Time Series – Run E4P1L7

Time Series – Run E4P1L7

Incident Time Series – Run E4P1L7
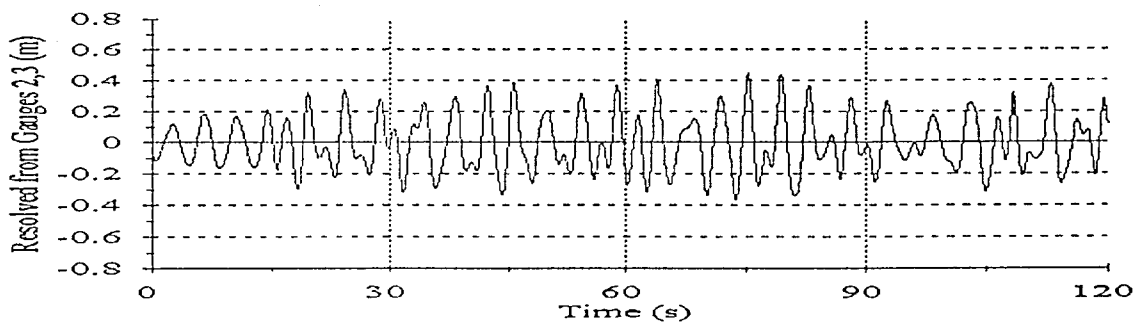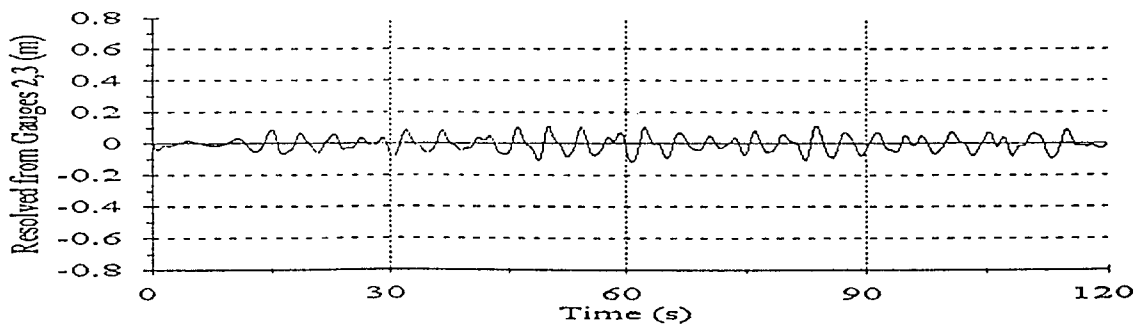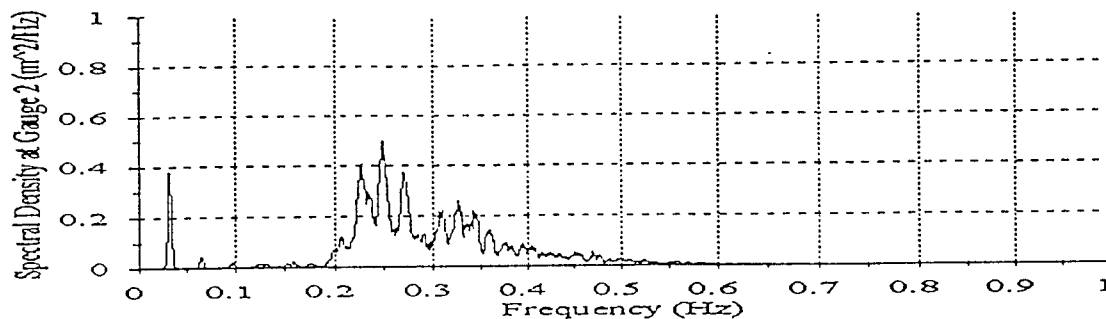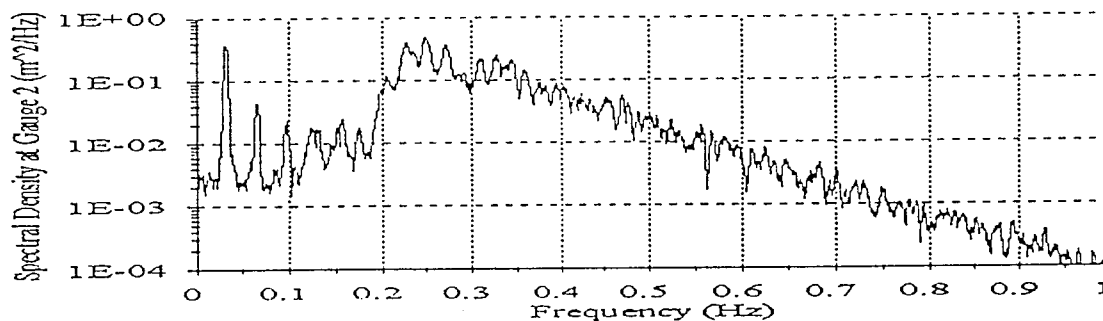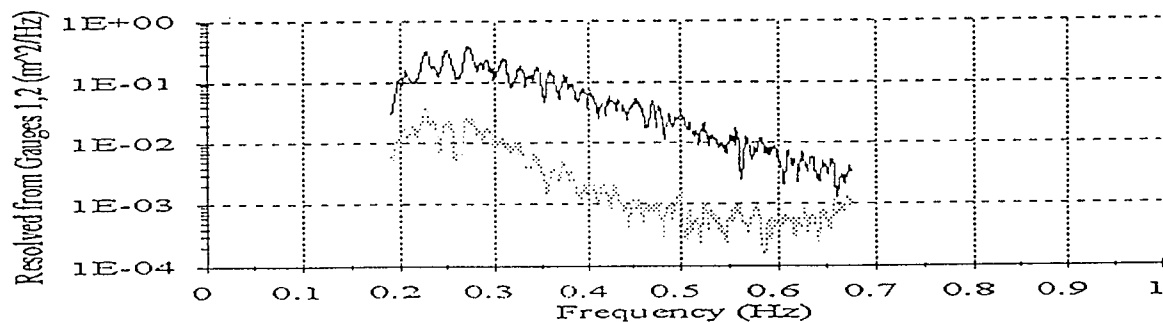

Reflected Time Series – Run E4P1L7

Composite Spectrum – Run E4P1L7

Composite Spectrum – Run E4P1L7

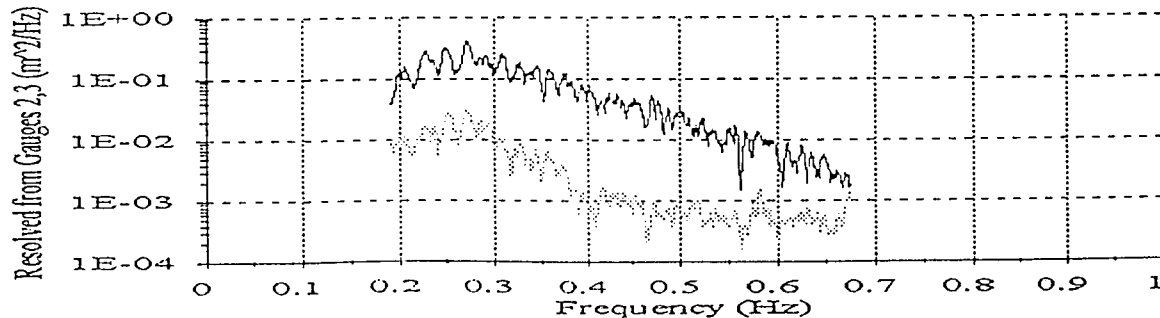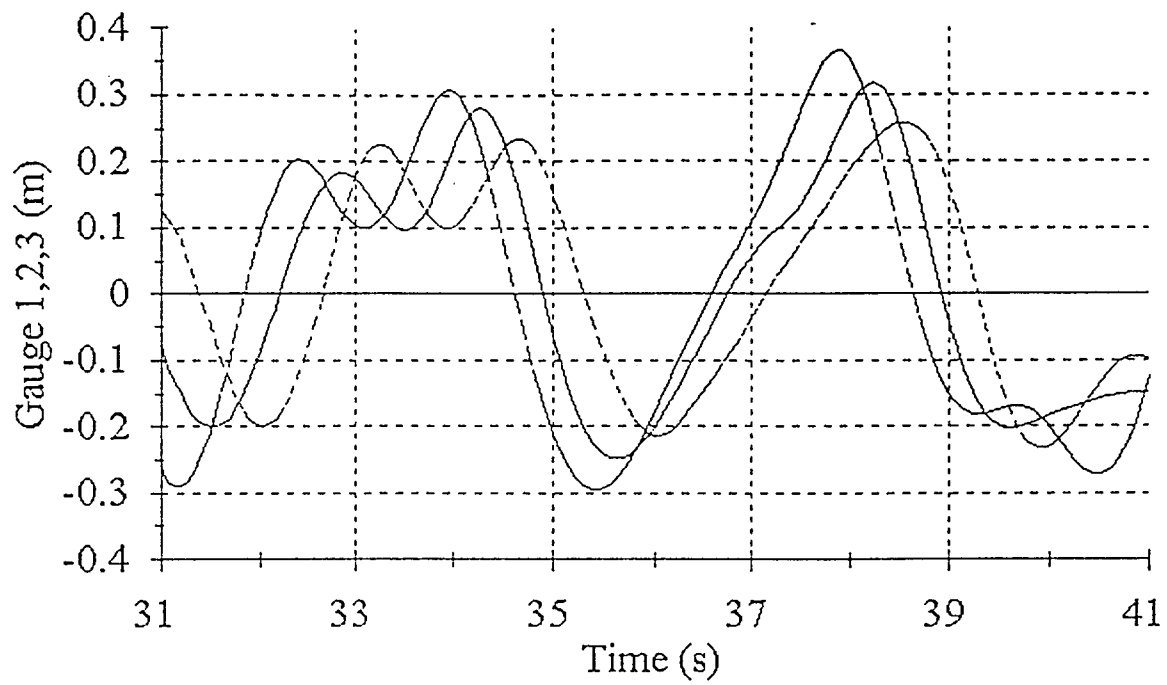Inc. and Ref. Spectra – Run E4P1L7

INCIDENT   REFLECTED

Inc. and Ref. Spectra – Run E4P1L7

INCIDENT   REFLECTED

Time Series - Run E4P1L7

Legend: — · GAUGE 1 —— GAUGE 2 --- GAUGE 3

APPENDIX D: References

Bruun, P. (1989). *Port Engineering*. Gulf Publishing Company, Houston, Texas, 507.

Burcharth, H. F. (1979). "The effects of wave grouping on on-shore structures." *Coast. Engrg.*, 2, 93-96.

Carstens, T., Torum, A., and Traetteberg, A. (1966). "The stability of rubble mound breakwaters against irregular waves." *Proc., 10th Int. Conf. on Coast. Engrg.*, ASCE, New York, N.Y., 958-971.

Chakrabarti, S. K. (1987). *Hydrodynamics of Offshore Structures*. Computational Mechanics Publications, Boston, Mass., 141.

Dean, R. G., and Dalrymple, R. A. (1984). *Water Wave Mechanics for Engineers and Scientists*. Prentice-Hall, Englewood Cliffs, New Jersey, 198.

Farlow, S. J. (1982). *Partial Differential Equations for Scientists and Engineers*. John Wiley & Sons, New York, 114.

Fassardi, C. (1993). "Effects of wave groups on breakwater damage," MSc thesis, Oregon State University, Corvallis, Oregon.

Goda, Y. (1985). *Random seas and design of maritime structures*. University of Tokyo Press, Tokyo, Japan, 26, 221, 299-303.

Goda, Y., and Suzuki, Y. (1976). "Estimation of incident and reflected waves in random wave experiments." *Proc., 15th Int. Conf. on Coast. Engrg.*, ASCE, New York, N.Y., 828-845.

Hall, K. R. (1994). "Influence of wave groups on stability of berm breakwaters." *J.*

Wtrwy., Port, Coast., and Oc. Engrg., 120(6), 630-636.

Hoffman, D., and Karst, O. J. (1975). "The Theory of the Rayleigh Distribution and Some of Its Applications." *Journal of Ship Research,* 19(3), 172-191.

Johnson, R. R., Mansard, E. P. D., and Ploeg, J. (1978). "Effects of wave grouping on breakwater stability." *Proc., 16th Int. Conf. on Coast. Engrg.,* Hamburg, Germany, 2228-2243.

Kimura, A. (1985). "The decomposition of incident and reflected random wave envelopes." *Coastal Engrg. in Japan,* 28, 59-69.

Kreyszig, E. (1983). *Advanced Engineering Mathematics.* Fifth Ed., John Wiley & Sons, New York, A-57.

Mase, H., and Iwagaki, Y. (1986). "Wave group analysis from statistical viewpoint." *Proc., Ocean Structural Dynamic Symposium.,* Oregon State University, Corvallis, Oregon, 145-157.

Medina, J. R., and Hudspeth, R. T. (1990). "A review of the analyses of ocean wave groups." *Coast. Engrg.,* 14, 515-542.

Medina, J. R., Fassardi, C., and Hudspeth, T. T. (1990). "Effects of wave groups on the stability of rubble mound breakwaters." *Proc., 22nd Int. Conf. on Coast. Engrg.,* ASCE, New York, N. Y., 1552-1563.

Medina, J. R., Hudspeth, R. T., and Fassardi, C. (1994). "Breakwater armor damage due to wave groups." *J. Wtrwy., Port, Coast., and Oc. Engrg.,* 120(2), 179-198.

Rye, H. (1980). "Wave parameter studies and wave groups." *Proc., Int. Conf. on Sea Climatology, Paris, 3-4 Oct. 1979.,* Editions Technip, Paris.

Rye, H. (1982). *Ocean Wave Groups*. Dept. of Marine Technology, Norwegian Institute of Technology, Trondheim, Norway, Report UR-82-18.

Sarpkaya, T., and Isaacson, M. (1981). *Mechanics of Wave Forces on Offshore Structures*. Litton Educational Publishing, New York, 491-492.

Shore protection manual. (1984). Dept. of the Army, Coast. Engrg. Res. Ctr., Wtrwy. Experiment Station, Vicksburg, Miss., 7:202-7:213.

Thornton, E. B., and Calhoun, R. J. (1972) "Spectral resolution of breakwater reflected waves." *J. of the Wtrwys., Harbors, and Coast. Engrg. Division,* 98(4), 443-460.

van der Meer, J. W. (1988). "Deterministic and probabilistic design of breakwater armor layers." *J. Wtrwy., Port, Coast., and Oc. Engrg.,* 114(1), 66-80.

Wolfram, S. (1991). *Mathematica*. Second Ed., Addison-Wesley Publishing Company, Inc., Redwood City, Ca., 572.

Woltring, H. J. (1986). "GCVSPL software package - A Fortran Package for generalized, cross-validatory spline smoothing and differentiation" *Adv. Eng. Software,* 8(2), 104.

APPENDIX E: Notation

$A(x,t)$ = wave envelope function

A_i = FFT coefficient at i^{th} wave gauge

a_{med} = the median of a

a_{mode} = most probable value of a

$\bar{a}_n$ = the average wave amplitude greater than a_n

a_{rms} = root mean square wave amplitude

a = incident wave amplitude

B_i = FFT coefficient at i^{th} wave gauge

b = reflected wave amplitude

c_1 = Goda-JONSWAP spectrum parameter defined in Eq. (B.2)

da = wave amplitude interval

dH = wave height interval

$d\xi$ = interval of ξ defined in Eq. (A.2e)

$E(\alpha')$ = expected value of α'

$erf(\cdot)$ = error function of $(\cdot)$

$erfc(\cdot)$ = complementary error function of $(\cdot)$

f = wave frequency

$\bar{f}$ = mean frequency of spectrum

$f_{max(min)}$ = maximum (minimum) cut-off frequency

58

f_p = peak frequency of spectrum

f_R = frequency ratio given by Eq. (B.8)

$G(a,z)$ = gamma function from APP. A

g = gravitational constant

H = wave height

$H(t)$ = wave height function at a fixed location

$H(x,t)$ = wave height function

$H(n\Delta t)$ = discrete wave height function at $x=0$

H_{med} = the median of H

H_{mode} = the most probable value of H

H_R = squared significant wave height ratio given by Eq. (B.5)

H_{rms} = root mean square wave height

H_s = significant wave height = $H_{1/3}$

$H_{s,full}$ = significant wave height of full spectrum

$H_{s,(k)}$ = significant wave height of the kth run

$H_{s,trunc}$ = significant wave height of truncated spectrum

H_1 = average of the wave heights

$H_{1/3}$ = average of the highest one-third of the wave heights

$H_{1/10}$ = average of the highest one-tenth of the wave heights

$H_{1/100}$ = average of the highest one-hundredth of the wave heights

h = water depth

j = $\sqrt{-1}$

K_D = armor layer stability coefficient

k (=$2\pi/L$) = wave number

L = wave length

$L_{max(min)}$ = maximum (minimum) wave length

m_0 = variance of the time series, zero-th spectral moment

m_1 = first spectral moment

n = percent or fraction of wave amplitudes greater than a_n

N = number of data points

N_s = stability number defined in Eq. (B.12)

$P(\cdot)$ = Rayleigh cumulative distribution function of ($\cdot$)

$p(\cdot)$ = Rayleigh probability density function of ($\cdot$)

$S_\eta(f)$ = Goda-JONSWAP spectrum defined by Eq. (B.1)

T = wave period

t = time

$U(\cdot)$ = Heaviside step function of ($\cdot$)

W = the median value of the mass distribution of rocks in the armor

W_L = large armor layer rock size

W_s = small armor layer rock size

X = complex valued FFT coefficient

x_i = position of ith wave gauge from wave maker

y = change of variable from Eq. (A.7)

α = envelope exceedance coefficient

α' = magnitude of the variation of wave energy above $H_{1/10}$

α_R = Rayleigh parameter

β = reflected wave phase

$\Gamma(a,z)$ = incomplete gamma function from APP. A

$\Gamma(a,z_0,z_1)$ = generalized incomplete gamma function from APP. A

γ = peak enhancement factor

ΔH_n = normalized measure of the variation of wave height

$\Delta \ell$ = wave gauge spacing

Δt = sampling time interval

ε = incident wave phase

ζ_i = reflected time series at i^{th} wave gauge

$\eta(x,t)$ = sea surface elevation

η_i = incident time series at i^{th} wave gauge

Θ = angle of the breakwater slope measured from horizontal

μ_a = average of the amplitude a

ξ = change of variable from Eq. (A.2e)

ρ_r = weight density of rock

ρ_w = weight density of water

σ = Goda-JONSWAP spectrum parameter defined in Eq. (B.3)

ϕ = constant phase shift applied to each realization

$\psi_{I(R)}$ = incident (reflected) spatial wave phase

$\omega \ (=2\pi/T)$ = circular wave frequency